Earth and Planetary Science Letters 299 (2010) 250–262

Contents lists available at ScienceDirect

Earth and Planetary Science Letters

journal homepage: www.elsevier.com/locate/epsl

A 35 Myr North American leaf-wax compound-specific carbon and hydrogen isotope record: Implications for C_4 grasslands and hydrologic cycle dynamics

Brett J. Tipple *, Mark Pagani

Department of Geology and Geophysics, Yale University, P.O. Box 208109, New Haven, CT 06520, USA

A R T I C L E I N F O

Article history:
Received 9 April 2010
Received in revised form 2 September 2010
Accepted 3 September 2010
Available online 29 September 2010

Editor: P. DeMenocal

Keywords:
carbon isotopes
hydrogen isotopes
Cenozoic
n-alkanes
Gulf of Mexico
DSDP Site 94

A B S T R A C T

Hydrology, source region, and timing of precipitation are important controls on the climate of the Great Plains of North America and the composition of terrestrial ecosystems. Moisture delivered to the Great Plains varies seasonally and predominately derives from the Gulf of Mexico/Atlantic Ocean with minor contributions from the Pacific Ocean and Arctic region. For this work, we evaluate long-term relationships for the past ~35 million years between North American hydrology, climate, and floral change, using isotopic records and average carbon chain lengths of higher plant *n*-alkanes from Gulf of Mexico sediments (DSDP Site 94). We find that carbon isotope values ($\delta^{13}C$) of *n*-alkanes, corrected for variations in the $\delta^{13}C$ value of atmospheric CO_2, provide minor evidence for contributions of C_4 plants prior to the Middle Miocene. A sharp spike in C_4 input is identified during the Middle Miocene Climatic Optimum, and the influence of C_4 plants steadily increased during the Late Miocene into the Pleistocene — consistent with other North American records. Chain-length distributions of *n*-alkanes, indicative of the composition of higher plant communities, remained remarkably constant from 33 to 4 Ma. However, a trend toward longer chain lengths occurred during the past 4 million years, concurrent with an increase in $\delta^{13}C$ values, indicating increased C_4 plant influence and potentially aridity. The hydrogen isotope values (δD) of *n*-alkanes are relatively invariant between 33 and 9 Ma, and then become substantially more negative (75‰) from 9 to 2 Ma. Changes in the plant community and temperature of precipitation can solely account for the observed variations in δD from 33 to 5 Ma, but cannot account for Plio-Pleistocene δD variations and imply substantial changes in the source region of precipitation and seasonality of moisture delivery. We posit that hydrological changes were linked to tectonic and oceanographic processes including the shoaling and closure of the Panamanian Seaway, amplification of North Atlantic Deep Water Production and an associated increase of meridional winds. The southerly movement of the Intertropical Convergence Zone near 4 Ma allowed for the development of a near-modern pressure/storm track system, driving increased aridity and changes in seasonality within the North American interior.

1. Introduction

Substantial changes in global climate and terrestrial ecology occurred over the past ~35 million years. Proxy CO_2 records indicate relatively low CO_2 concentrations during the last 24 Ma and suggest that major glaciations and patterns of global warming were driven by relatively small changes in atmospheric CO_2 and tectonically driven changes in ocean circulation and planetary wind patterns (DeConto and Pollard, 2003; Driscoll and Haug, 1998; Lawver and Gahagan, 2003; Osborne and Beerling, 2006; Pagani et al., 2005; Rea, 1994; Ruddiman et al., 1989). Particularly important tectonic climate drivers of the last 35 Myr include deepening of the Drake Passage, development of large ice sheets on Antarctica, uplift in the Himalayas and Andes, and closure of the Panamanian Seaway. These events drove fundamental changes in regional and global hydrological cycles prompting variations in temperature and seasonality of precipitation. Long-term terrestrial ecological changes associated with changes in climate are also known to have occurred including loss of forests and expansion of grasslands during the latest Oligocene to early Miocene (Jacobs et al., 1999), evolution in large mammal physiology (Janis et al., 2000), and the global expansion of C_4 grasses in the late Miocene (Cerling et al., 1997; Strömberg, 2005).

Determining whether or not CO_2 change was the primary driver of ecological change is the source of a protracted debate. The C_4 photosynthetic pathway is adapted for specific environmental conditions, and in its various forms, the terrestrial C_4 photosynthetic pathway has evolved at least 45 times in separate lineages (Sage, 2004) in order to enhance photosynthetic efficiency under low atmospheric CO_2/O_2 ratios, elevated light, high temperature, and water-limited conditions. Thus, the early origins and distribution of

---

* Corresponding author. Current address: Department of Biology, University of Utah, Salt Lake City, UT, USA. Tel.: +1 801 587 3545; fax: +1 801 581 4665.
E-mail addresses: brett.tipple@utah.edu (B.J. Tipple), mark.pagani@yale.edu (M. Pagani).

0012-821X/$ – see front matter © 2010 Elsevier B.V. All rights reserved.
doi:10.1016/j.epsl.2010.09.006

terrestrial C_4 plants reflect a record of climatic change (Tipple and Pagani, 2007). Terrestrial C_4 photosynthesis, characteristic of tropical grasses, is not a single photosynthetic pathway, but rather a general CO_2 concentrating model with several distinct biochemical variations and anatomical modifications. The biochemistry and physiology of C_4 photosynthesis is understood (Sage, 2004), however, details of terrestrial C_4 plant evolution, and the origin and large-scale expansion of the C_4 pathway remain enigmatic (Edwards et al., 2010; Osborne, 2008; Tipple and Pagani, 2007).

Differences in C_3 and C_4 plant physiologies result in distinct stable carbon isotope compositions ($\delta^{13}C$) that are useful for ecosystem and dietary reconstructions. Average $\delta^{13}C$ values of modern C_3 and C_4 bulk plant material are −28‰ and −14‰, respectively (Cerling et al., 1997; Deines, 1980). Temporal patterns of C_4 plant abundances have been evaluated using end-member carbon isotopic values and $\delta^{13}C$ records of fossil herbivore teeth (Cerling et al., 1997), pedogenic carbonate nodules and soil organic matter (Fox and Koch, 2003, 2004; Latorre et al., 1997; Quade et al., 1989), and leaf-wax lipids extracted from marine sediments (Feakins et al., 2005, 2007; Freeman and Colarusso, 2001; Huang et al., 2001). Compilations of fossil teeth suggest that C_4 niches rapidly expanded and became an important component of herbivore diets across the low and middle latitudes during the Late Miocene/Pliocene (Cerling et al., 1997). More recent studies suggest regional differences in the temporal expression of C_4 grassland evolution (Passey et al., 2002; Segalen et al., 2006; Tipple and Pagani, 2007). Due to the physiological advantages that C_4 plants possess under low atmospheric CO_2/O_2 concentrations, the widespread expansion of C_4 plants between 8 and 4 Ma has been attributed to a large decline in pCO_2 (Cerling et al., 1997). However, alkenone-based pCO_2-proxy records show no support for a decrease in CO_2 concentration before or during C_4 expansion in the Late Miocene (Pagani et al., 1999). While variations in Miocene pCO_2 are likely (Kurschner et al., 2008), all available proxy records suggest that CO_2 concentration during the Miocene was below 500 ppmv — the theoretical threshold that favors C_4 over the C_3 pathway (Ehleringer et al., 1997).

Evidence for local and regional expansions of C_4 grasslands during the Late Miocene is compelling (Cerling et al., 1997), but there is no consensus regarding its cause. Numerous studies have documented changes in tectonics (Dettman et al., 2001; Ehleringer et al., 1997; Ruddiman et al., 1989; Sepulchre et al., 2006), seasonality of precipitation (Quade et al., 1989), aridity (Latorre et al., 1997; Osborne, 2008), and fire regime (Keeley and Rundel, 2005; Osborne and Beerling, 2006) preceding and accompanying C_4 expansion, thus implicating regional and/or local environmental forcing factors over global changes in CO_2.

Proxy records indicate that CO_2 concentrations during the early Eocene ranged between ~1000 and 2000 ppmv and then rapidly decreased during the Oligocene, reaching modern levels by the beginning of the Miocene (Lowenstein and Demicco, 2006; Pagani et al., 2005; Pearson and Palmer, 2000). Low atmospheric CO_2 conditions during the latest Oligocene should have favored C_4 photosynthesis, and molecular phylogenies place the earliest origins of C_4 grasses during the Oligocene between 25 and 32 million years ago (Bouchenak-Khelladi et al., 2009; Christin et al., 2007, 2008; Kellogg, 2001; Vincentini et al., 2008). Low CO_2/O_2 conditions is arguably a precondition for the onset of the C_4 photosynthetic pathway, however, it remains unclear why the prevalence of C_4 grasses as ecosystem dominants was restricted prior to the late Miocene/Pliocene. Fossil evidence from North America (MacGinitie, 1962) supports the presence of C_4 plants during the Middle Miocene (16–11 Ma). Geochemical evidence for a Middle Miocene appearance in North America is limited, but growing (Fox and Koch, 2003, 2004; Passey et al., 2002).

Fossil tooth and soil carbonate isotope records provide sparse local and regional C_4 plant histories from various continents due to the nature of terrestrial sedimentation (Koch, 1998). In contrast, marine records provide temporally long and spatially integrated records of the terrestrial environment, and often preserve a better terrestrial plant signature than paleosols (Freeman and Colarusso, 2001). Marine sedimentation is influenced by riverine influx, winds, and ocean currents to deliver terrestrial materials. Changes in geography, topography, wind patterns, and marine currents could substantially impact the delivery of terrestrial organic material to deep-sea locations and must be considered when evaluating terrestrial records from marine sediments.

The $\delta^{13}C$ values of *normal*-alkanes (*n*-alkanes) and other leaf waxes from C_3 and C_4 plants average $-33.1 \pm 2.3‰$ (1σ) and $-21.7 \pm 2.4‰$ (1σ), respectively (Bi et al., 2005; Chikaraishi and Naraoka, 2003; Chikaraishi et al., 2004; Collister et al., 1994; Lockheart et al., 1997; Rommerskirchen et al., 2006; Vogts et al., 2009), and have been extracted from marine and lacustrine sediments to reconstruct ancient African and Indian C_3/C_4 ecosystem variations (Feakins et al., 2005, 2007; Freeman and Colarusso, 2001; Huang et al., 2007; Russell et al., 2009; Schefuss et al., 2003; Tierney et al., 2010). To date, North and South American marine records have not been evaluated. In addition carbon isotope records, hydrogen isotopic compositions of leaf-wax lipids potentially record plant community changes (Smith and Freeman, 2006), given that the apparent hydrogen fractionation between *n*-alkane and source water of leaf waxes ($\varepsilon_{alk-water}$) differs between C_3 dicots, C_4 grasses, and C_3 grasses (Chikaraishi and Naraoka, 2003; Smith and Freeman, 2006), with $\varepsilon_{alk-water}$ defined as:

$$\varepsilon_{alk-water} = \left(\frac{R_{alk}}{R_{water}} - 1\right) \times 1000 \tag{1}$$

where R_{alk} and R_{water} represent the D/H of *n*-alkane and water, respectively. Thus, apparent hydrogen fractionations are influenced by rates of evapotranspiration, the plant's specific water-use efficiency, and the hydrogen isotope composition of source water used during photosynthesis (Hou et al., 2007; Pedentchouk et al., 2008; Roden et al., 2000). As a result, interpretations of D/H records require consideration of both hydrological conditions and plant community variations.

In general, C_4 grasses also produce longer-chain *n*-alkanes compared to C_3 plants (Rommerskirchen et al., 2006) and increased seasonal temperature and decreased precipitation have been shown to correlate to increased *n*-alkane chain length in a variety of plant species (Hughen et al., 2004; Schefuss et al., 2003). While compound distribution data in the sedimentary record is not specifically indicative of C_3 and C_4 plants, it offers cursory evidence of plant community changes.

In this study, we present molecular isotope records and estimates of C_3 and C_4 contributions delivered to marine sediments in the Gulf of Mexico (DSDP Site 94) during the last 35 million years. We focus our analysis on long-chained, odd-carbon number *n*-alkanes (*n*-C_{25} to *n*-C_{33}). The resulting *n*-alkane $\delta^{13}C$ record is then used to assess the character of C_4 plant expansion on North America, while *n*-alkane δD and compound distributions are used to interpret hydrological conditions. This coupled *n*-alkane approach provides a continental-scale record of the paleohydrological cycle and its influences on biology over long time scales.

2. Methods

2.1. Sample location and materials

The Mississippi River is the primary source of sedimentary material entering the Gulf of Mexico (Hedges and Parker, 1976; Trefry et al., 1994) and drains an area of ~3.0×10^6 km^2 (Canfield, 1997), contributing 70–90% of fresh water entering the Gulf of Mexico (Dinnel and Wiseman, 1986). The Mississippi outlet has roughly maintained its present position from the Middle Miocene to the Present (Galloway et al., 1991; Winker, 1981). During the Early Miocene, the primary North American input to the Gulf of Mexico was near the present-day western Louisiana (Sloane, 1971), and near southern Texas/Mexico during the Oligocene (Alzaga-Ruiz et al., 2009; Kiatta, 1971). Nonetheless, the Mississippi River has drained the North American continental interior the entire interval of interest in this study.

For this study, we analyzed lipids extracted from 159 samples from DSDP Leg 10, Site 94 (24°31.64′N, 88°28.16′W) (Fig. 1). Site 94 is centrally located in the Gulf of Mexico, approximately 500 km south of the mouth of the Mississippi River on the base of the Yucatan platform continental slope at a depth of 1793 m (Fig. 1). Carbonate marine organisms and terrigenous clays dominate late Cenozoic sediments (Worzel et al., 1971). Terrigenous material was sourced from the north and west given surrounding paleodrainages with organic carbon making up 0.1 to 0.3 wt.% of the sediments (Boyce, 1973). Sediments were dated biostratigraphically (Hay, 1973) and correlated to the standard Cenozoic geomagnetic polarity time scale (GPTS) (Berggren et al., 1995).

2.2. Extraction, separation, and analytical methods

Organic material was extracted from dry, powdered sediment samples (100–150 g) with an automated solvent extractor (ASE 300) using dichloromethane at 150 °C and 1500 psi. Total lipid extracts were concentrated under a stream of purified nitrogen using a Zymark Turbovap II evaporator, transferred to 4 ml vials, and further evaporated under a gentle stream of N_2 gas. Extracts were then separated by column chromatography using 4 g deactivated silica gel (70–230 mesh) in an ashed Pasteur pipette, and eluted with 2 ml hexane to obtain the aliphatic hydrocarbons. *N*-alkanes were further purified from cyclic and branched alkanes using urea adduction following Wakeham and Pease (1992).

Compound abundances were determined using a Thermo Trace 2000 gas chromatograph (GC) fitted with a programmable-temperature vaporization injector and flame ionization detector (FID). A fused silica, DB-1 phase column (60 m × 0.25 mm I.D., 0.25 μm film thickness) was used with helium as the carrier at a flow of 2 ml/min. GC oven temperature program utilized was 60–320 °C at 10 °C/min with an isothermal for 30 min. *N*-alkanes were identified through comparison of elution times with known *n*-alkane standards.

2.3. Molecular distributions of *n*-alkanes

Individual *n*-alkane peak areas were calculated and carbon preference indices (CPI) were calculated to quantify the abundance of odd-over-even *n*-alkanes following Marzi et al. (1993):

$$CPI = \frac{(C_{23}+C_{25}+C_{27}+C_{29}+C_{31}+C_{33})+(C_{25}+C_{27}+C_{29}+C_{31}+C_{33}+C_{35})}{2(C_{24}+C_{26}+C_{28}+C_{30}+C_{32}+C_{34})}. \tag{2}$$

Changes in average higher plant chain length (AHPCL) were calculated using the following relationship:

$$AHPCL = \frac{(A_{27}(27))+(A_{29}(29))+(A_{31}(31))}{(A_{27}+A_{29}+A_{31})} \tag{3}$$

where A corresponds to the area of the individual *n*-alkane peak from the chromatograph trace.

2.4. Compound-specific carbon and hydrogen isotope analysis

Isotope analyses were performed using a Thermo Trace 2000 GC coupled to a Finnigan MAT 253 isotope ratio mass spectrometer interfaced with a GC–C III combustion system. Hydrogen isotope analyses were performed using a Thermo Trace 2000 GC coupled to a Finnigan MAT 253 isotope ratio mass spectrometer with a high temperature conversion system for δD analysis. GC column, carrier flow, and ramp conditions for both $\delta^{13}C$ and δD analyses were identical to the above. For δD analysis, the H_3^+ factor was determined daily prior to standard calibration and sample analysis.

Isotopic compositions are calculated following:

$$\delta = \left[\frac{R_{samp}-R_{std}}{R_{std}}\right] \times 1000 \tag{4}$$

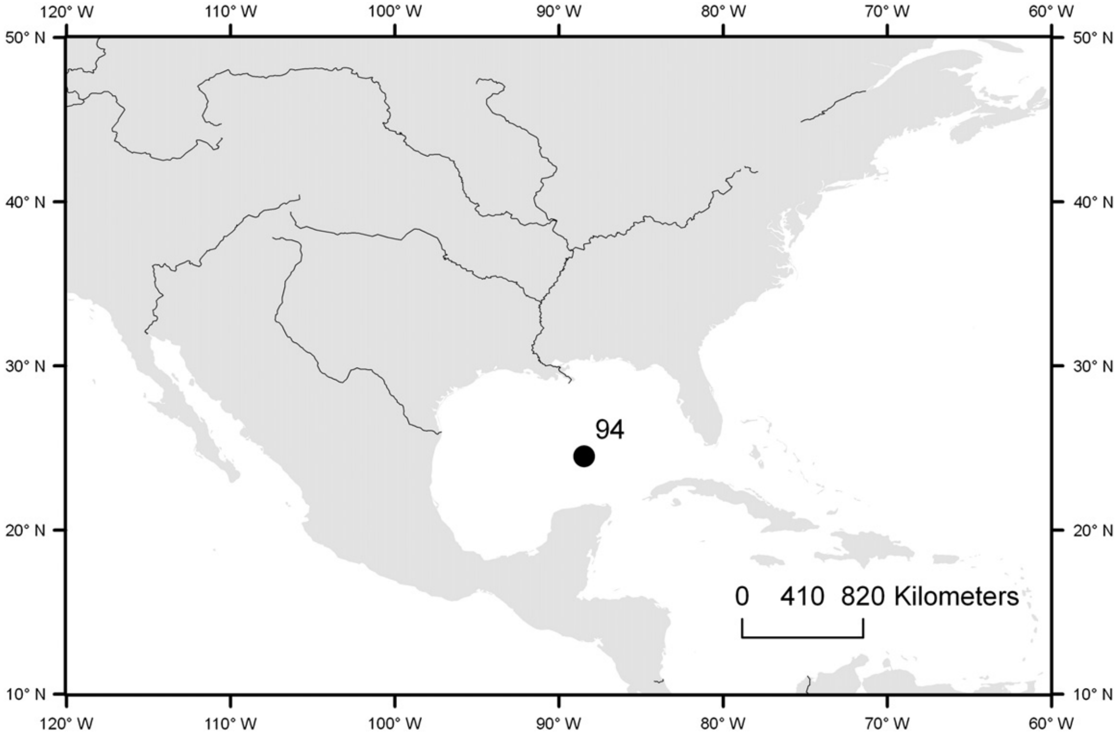

Fig. 1. Location map with Mississippi River and other major rivers. DSDP Site 94 (black circle) is located in the central Gulf of Mexico.

Table 1
DSDP Site 94 *n*-alkane distributions, δ^{13}C (‰, VPDB) and δD values (‰, VSMOW).

Sample information						Compound distributions		δ^{13}C$_{CO2}$	δ^{13}C		δD	
Site	Core	Sect	Start (cm)	End (cm)	Age (Ma)	CPI	AHPCL		*n*-C$_{29}$	*n*-C$_{31}$	*n*-C$_{29}$	*n*-C$_{31}$
94	1	2	30	36	0.02	3.15	29.69					
94	1	2	100	106	0.03	2.85	29.54	−6.65	−29.35	−28.40	−202 ± 5	−198 ± 4
94	2	1	43	49	2.13	3.31	29.68	−6.53	−28.26	−28.47		
94	2	1	93	99	2.16	2.85	29.59	−6.53		−28.94		
94	2	2	43	49	2.23	2.68	29.67	−6.51	−30.11	−29.15	−220	−214
94	2	2	92	98	2.27	3.29	29.64	−6.50	−29.54	−29.02		
94	2	3	43	48	2.34	3.04	29.70					
94	2	3	111	117	2.39	2.74	29.60	−6.46	−29.07 ± 0.32	−28.43 ± 0.20		
94	2	4	52	58	2.45	2.90	29.49	−6.44	−29.17 ± 0.04	−28.42 ± 0.06		
94	2	4	101	107	2.48	2.79	29.62	−6.43	−28.61 ± 0.24	−27.98 ± 0.18		
94	2	5	45	50	2.55	2.95	29.67	−6.43	−28.79	−28.11		
94	2	5	85	92	2.58	2.54	29.51	−6.43	−29.52	−28.66		
94	2	6	52	58	2.66	2.91	29.61	−6.42	−29.69	−28.87		
94	2	6	112	117	2.70	2.99	29.60	−6.42	−29.20 ± 0.08	−28.39 ± 0.05		
94	3	1	53	59	3.09	2.61	29.40					
94	3	1	90	97	3.09	2.82	29.38	−6.36	−30.17 ± 0.04	−29.25 ± 0.08		
94	3	2	44	50	3.11	2.63	29.49	−6.37	−30.18	−29.20		
94	3	2	93	99	3.12	2.29	29.55	−6.37		−29.02 ± 1.13		
94	3	3	45	51	3.13	3.04	29.64	−6.37	−28.39 ± 0.80	−27.33 ± 0.70		
94	3	3	95	101	3.14	2.78	29.61	−6.37	−28.83 ± 0.39	−27.39 ± 0.37		
94	3	4	58	64	3.16	2.75	29.56	−6.37	−29.01 ± 0.20	−27.89 ± 0.09		
94	3	4	114	121	3.17	3.09	29.46					
94	3	5	24	30	3.17	2.93	29.67	−6.37	−29.35 ± 0.17	−28.21 ± 0.31		
94	3	5	93	99	3.18	2.77	29.62	−6.37	−29.89 ± 1.20	−28.89 ± 0.71		
94	3	6	53	60	3.26	2.73	29.27					
94	3	6	97	104	3.27	2.68	29.51	−6.37	−29.50	−28.63		
94	4	1	52	58	3.88	2.52	29.48	−6.31	−29.45	−28.98		
94	4	1	112	118	3.89	2.85	29.41	−6.31	−30.26	−29.66		
94	4	2	53	60	4.07	2.08	29.36					
94	4	2	95	100	4.09	2.28	29.43					
94	4	3	29	34	4.11	2.58	29.49	−6.24	−29.34	−28.70		
94	4	3	127	132	4.14	2.92	29.38	−6.24	−29.42	−29.70 ± 0.09		
94	4	4	66	74	4.17	2.27	29.25					
94	4	4	118	124	4.18	2.47	29.30					
94	4	5	42	47	4.20	2.76	29.43					
94	4	5	92	98	4.22	2.37	29.32					
94	4	6	42	49	4.25	2.64	29.37					
94	5	1	26	32	5.15	2.17	29.28					
94	5	1	79	85	5.17	2.72	29.45					
94	5	1	125	130	5.18	2.75	29.43					
94	5	2	58	64	5.21	2.12	29.44	−6.34	−29.89 ± 0.02	−29.50 ± 0.21		
94	5	2	115	121	5.22	2.35	29.41	−6.34	−30.02 ± 0.19			
94	5	3	46	52	5.25	2.64	29.46	−6.34	−29.67 ± 0.22	−29.15 ± 0.40		
94	5	3	86	92	5.26	2.57	29.38	−6.34	−29.60 ± 0.14			
94	5	4	47	53	5.29	2.30	29.36					
94	5	4	98	103	5.31	2.61	29.43	−6.33	−29.63	−28.54		
94	5	4	135	140	5.32	2.72	29.32					
94	5	5	48	53	5.34	2.74	29.47	−6.33	−29.12 ± 0.13	−28.33 ± 0.26		
94	5	5	100	105	5.35	2.63	29.27					
94	5	6	57	62	5.38	2.79	29.35	−6.32	−29.13	−27.48		
94	5	6	100	104	5.39	2.77	29.38	−6.32	−30.11	−28.86		
94	6	4	99	104	6.46	2.45	29.28	−6.20	−28.91 ± 0.35	−29.62 ± 0.31		
94	6	4	134	139	6.47	2.55	29.28					
94	6	5	10	15	6.47	2.55	29.32	−6.20	−30.52	−31.03		
94	6	5	56	60	6.49	3.00	29.38	−6.20	−30.22 ± 0.05	−29.22 ± 0.01		
94	6	5	90	95	6.50	3.10	29.41	−6.19	−29.73 ± 0.06	−29.16 ± 0.08		
94	6	5	129	133	6.51	3.49	29.39					
94	6	6	18	23	6.52	3.43	29.44	−6.19	−30.18 ± 0.33	−29.53 ± 0.58		
94	6	6	28	35	6.52	2.99	29.43	−6.19	−30.20 ± 0.04	−29.21 ± 0.05		
94	6	6	46	51	6.53	3.28	29.45	−6.19	−30.12 ± 0.18	−29.36 ± 0.20	−189 ± 4	−192 ± 6
94	6	6	97	102	6.54	2.34	29.15	−6.19	−28.19 ± 0.41	−28.20 ± 0.10		
94	6	6	119	124	6.55	3.04	29.44	−6.19	−30.28 ± 0.18	−30.01 ± 0.22		
94	6	6	139	145	6.55	3.39	29.36	−6.19	−30.39 ± 0.05	−29.86 ± 0.02	−193 ± 6	
94	7	1	108	113	7.34	2.34	29.28	−6.10	−30.92 ± 1.06	−30.92 ± 1.14		
94	7	1	118	123	7.34	2.02	29.33	−6.10	−30.45	−30.64	−162 ± 1	−168 ± 1
94	7	1	135	140	7.35	2.87	29.55	−6.09	−29.92 ± 0.13	−29.21 ± 0.27	−185	−184
94	7	2	29	34	7.36	3.10	29.31	−6.09	−29.87	−29.15		
94	7	2	51	57	7.37	3.04	29.39	−6.09	−29.65 ± 0.18	−29.05 ± 0.20		
94	7	2	86	92	7.38	2.82	29.40	−6.09	−29.53 ± 0.05	−30.31 ± 0.21		
94	7	2	102	105	7.38	2.51	29.31	−6.09	−30.23	−29.91		
94	7	2	131	135	7.39	2.78	29.32	−6.09	−28.67		−186 ± 2	−192 ± 2

(continued on next page)

Table 1 (*continued*)

Sample information						Compound distributions		$\delta^{13}C_{CO2}$	$\delta^{13}C$		δD	
Site	Core	Sect	Start (cm)	End (cm)	Age (Ma)	CPI	AHPCL		*n*-C_{29}	*n*-C_{31}	*n*-C_{29}	*n*-C_{31}
94	7	3	20	26	7.40	2.87	29.32	−6.09	−29.99 ± 0.19	−29.20 ± 0.14	−204	−206
94	7	3	65	70	7.42	2.63	29.26	−6.09	−29.63 ± 0.28	−29.05 ± 0.27	−198	−199
94	7	3	92	97	7.42	2.38	28.96	−6.08	−29.69 ± 0.07	−29.93 ± 0.25		
94	7	3	135	140	7.44	3.15	29.29	−6.08	−29.67 ± 0.02	−29.39 ± 0.24		
94	7	4	48	53	7.46	3.19	29.28	−6.08	−29.86 ± 0.01	−29.26 ± 0.04		
94	7	4	88	93	7.47	2.62	29.27	−6.08	−29.58 ± 0.01	−29.81 ± 0.30	−163 ± 3	−171 ± 3
94	7	4	124	131	7.48	3.11	29.47	−6.08	−29.92 ± 0.63	−29.92 ± 0.50	−170 ± 1	−174 ± 1
94	7	5	26	31	8.26	3.22	29.40	−5.95	−29.27 ± 0.10	−28.74 ± 0.04		
94	7	5	86	92	8.31	2.99	29.26	−5.95	−29.71 ± 0.45	−29.88 ± 0.22		
94	7	5	135	140	8.35	3.07	29.36	−5.95	−29.36 ± 0.02	−28.60 ± 0.27		
94	8	2	40	47	8.63	2.96	29.42	−5.94	−29.77 ± 0.14	−29.52 ± 0.34		
94	8	2	95	100	8.67	2.21	29.37	−5.94	−30.15	−30.06	−155 ± 2	−160 ± 1
94	8	3	22	29	8.73	2.08	29.21	−5.95	−30.09 ± 0.05	−29.80 ± 0.00		
94	8	3	67	72	8.76	2.61	29.30	−5.95	−30.20 ± 0.07	−29.63 ± 0.01		
94	8	3	125	131	8.81	2.57	29.35	−5.95	−29.58 ± 0.10	−29.71 ± 0.08	−164 ± 5	−169 ± 5
94	8	4	96	102	8.91	2.12	29.35	−5.96	−29.40 ± 0.01	−29.65 ± 0.06	−156 ± 3	−164 ± 2
94	8	5	50	54	8.99	3.21	29.45	−5.96	−30.93 ± 1.56	−29.84 ± 0.14		
94	8	5	101	106	9.03	2.52	29.57	−5.96	−29.49 ± 0.06	−29.67 ± 0.04	−144 ± 3	−154 ± 1
94	8	5	136	141	9.05	2.98	29.51	−5.96	−29.38 ± 0.47	−29.21 ± 0.42		
94	9	1	11	17	15.39	2.75	29.19	−5.26	−26.17 ± 0.69	−25.19 ± 0.48		
94	9	1	49	54	15.46	2.48	29.07	−5.27	−26.57 ± 0.31	−24.83		
94	9	1	79	86	15.51	2.83	29.29	−5.25	−28.14 ± 0.41	−26.74 ± 0.59	−167 ± 1	−158 ± 1
94	9	1	100	106	15.55	2.01	29.10	−5.26	−28.19 ± 0.01	−28.94 ± 0.34		
94	9	1	131	136	15.60	3.16	29.30					
94	9	2	14	19	15.66	2.54	29.22	−5.27	−28.65 ± 0.33	−28.38 ± 0.04		
94	9	2	43	49	15.71	3.16	29.22	−5.27	−28.50 ± 0.01	−28.11 ± 0.09		
94	9	3	15	20	15.91	3.14	29.39					
94	9	3	44	51	15.96	2.74	29.37	−5.30	−29.19 ± 0.33	−28.61 ± 0.33	−181 ± 1	−199 ± 0
94	9	3	81	86	16.03	2.91	29.43	−5.31	−28.21 ± 0.15	−27.58 ± 0.21		
94	9	3	117	123	16.09	2.00	29.21	−5.32	−27.92 ± 0.03	−27.82 ± 0.04	−145 ± 3	−153 ± 3
94	9	4	43	47	16.22	3.46	29.25					
94	9	5	27	32	16.45	2.96	29.14	−5.34	−28.38 ± 0.10	−27.73 ± 0.20		
94	9	5	85	92	16.55	2.35	29.22	−5.34	−28.56 ± 0.07	−28.61 ± 0.07	−151 ± 2	−162 ± 2
94	9	5	114	118	16.60	3.54	29.25	−5.35	−29.06 ± 0.03	−28.48 ± 0.07		
94	9	6	26	32	16.71	3.03	29.16	−5.36	−29.09 ± 0.17	−27.73 ± 0.22		
94	9	6	95	100	16.82	3.60	29.34	−5.39	−29.35 ± 0.26	−28.06 ± 0.20	−178 ± 7	−188 ± 8
94	9	6	131	136	16.89	3.39	29.31	−5.40	−29.57 ± 0.27	−29.22 ± 0.21	−174 ± 5	−186 ± 3
94	10	2	66	71	21.64	2.53	29.39	−5.88	−28.90 ± 0.03	−29.65 ± 0.01	−153 ± 2	−158 ± 1
94	10	3	52	57.5	21.85	2.50	29.51	−5.85	−30.29 ± 0.09	−30.24 ± 0.03	−153 ± 1	−163 ± 5
94	11	5	92	97	28.47	2.82	29.45	−6.31	−28.68	−29.58 ± 0.55	−156	−162
94	12	1	83	89	29.00	2.44	29.31	−6.31	−29.00 ± 0.09	−29.74 ± 0.18		
94	12	4	88	93	29.84	2.04	29.33	−6.29	−29.08 ± 0.15	−30.17 ± 0.36	−151	−156
94	13	2	79	85	30.93	2.97	29.50	−6.06	−30.09 ± 0.09	−30.67 ± 0.47		
94	13	2	88	92	30.94	2.49	29.41	−6.06	−28.84 ± 0.02	−29.48 ± 0.13	−156 ± 6	−159 ± 8
94	13	3	125	131	31.29	2.49	29.40	−6.04	−28.82 ± 0.15	−29.56 ± 0.10		
94	14	2	82	87	31.91	2.34	29.41					
94	14	2	136	140	31.94	2.87	29.35					
94	14	3	47	53	31.98	2.54	29.40					
94	14	3	90	96.5	32.01	2.45	29.62					
94	16	1	116	120	32.55	2.50	29.22					
94	16	2	54	59	32.61	2.00	29.26					
94	16	2	114	119	32.65	2.02	29.28					
94	16	3	57	62	32.71	3.43	29.55					
94	16	3	92	98	32.73	3.01	29.44					

where R represents the $^{13}C/^{12}C$ and D/H abundance ratio, and R_{samp} and R_{std} represent the sample and standard, respectively. $\delta^{13}C$ and δD values are expressed relative to Vienna Pee Dee belemnite (VPDB) and Vienna Standard Mean Ocean Water (VSMOW), respectively, based on an in-house reference gas calibrated against OzTech standard gases.

Peaks were quantified using an individual baseline algorithm for both carbon and hydrogen measurements. Individual *n*-alkane isotope ratios were corrected to *n*-alkane standards (for $\delta^{13}C$, C_{20}, C_{25}, C_{27}, C_{30}, and C_{38} of known isotopic ratio and for δD, 'Mix A' supplied by Arndt Schimmelman, Indiana University) analyzed daily at several concentrations. In addition, 5α-androstane of known isotopic composition was co-injected to confirm standard corrections were appropriate. Precision in isotope determinations for *n*-alkanes was ±0.61‰ and ±6‰ for $\delta^{13}C$ and δD, respectively.

3. Results

3.1. Molecular distributions of *n*-alkanes

The CPI values for Site 94 range from 1.3 to 3.6 (Table 1, Fig. 2a). CPI does not correlate with sample depth/age suggesting no down-core diagenesis/alteration or hydrocarbon migration within Site 94 sediments. Nonetheless, CPI values near 1 could represent samples influenced by algae/bacterial inputs and/or bacterial oxidation. Accordingly, we limit our isotope analyses to only the 139 samples with CPI values greater than 2.0.

Site 94 AHPCL values range from 28.96 to 29.70 and higher plant *n*-alkane peak areas and AHPCL are shown in Table 1 and Figure 2b. Small variations in AHPCL are apparent from 35 to 4 Ma of the Site 94 record, and markedly increase after 4 Ma (Fig. 2b).

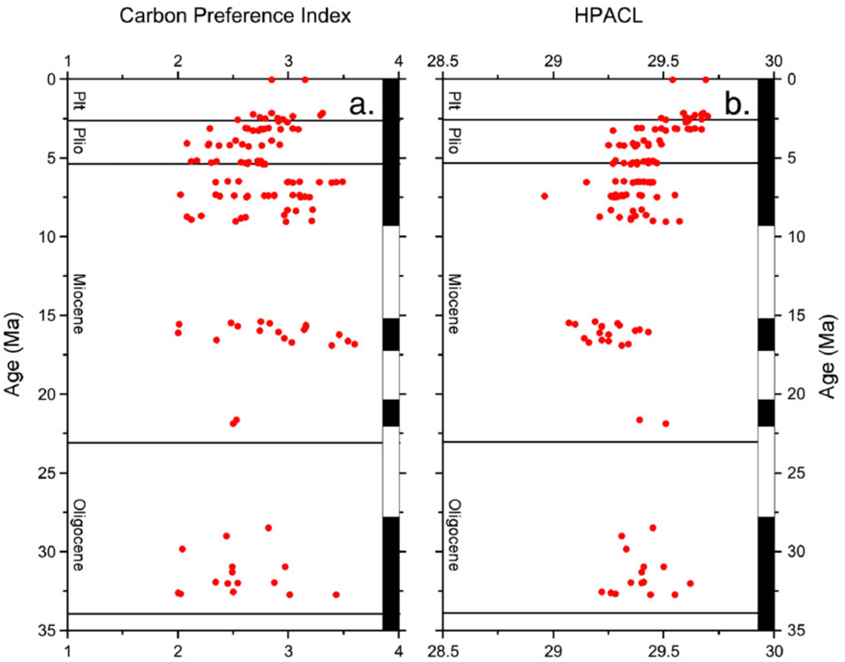

Fig. 2. (a) Carbon Preference Index (CPI) for Site 94 *n*-alkanes. (b) Average higher plant chain lengths (AHPCL) from Site 94 *n*-alkane distributions.

3.2. N-alkane carbon isotope ratios

$\delta^{13}C$ values of *n*-C_{29} and *n*-C_{31} ($\delta^{13}C_{n\text{-}C29}$ and $\delta^{13}C_{n\text{-}C31}$, respectively) are similar and vary in concert (Table 1, Fig. 3), suggesting a similar organic source (Table 1). Terrestrial *n*-alkanes are ^{13}C-enriched in the earliest Oligocene (31.3 Ma) and trend toward more negative values through 30.9 Ma (Fig. 3). For the remainder of the Early Oligocene, $\delta^{13}C_{n\text{-}C29}$ and $\delta^{13}C_{n\text{-}C31}$ values remain invariant and relatively positive. Following a 32-meter drill core gap, Early Miocene $\delta^{13}C_{n\text{-}C29}$ values are more negative than those in the Oligocene (Fig. 3a), and become increasingly more positive by 21.6 Ma. Middle Miocene $\delta^{13}C_{n\text{-}C29}$ and $\delta^{13}C_{n\text{-}C31}$ values are relatively constant and then rapidly increase by 2–4‰ between 15.4 and 15.6 Ma — the most ^{13}C-enriched values of the Cenozoic Gulf of Mexico record. Following a 34-meter sediment core gap between 15.4 and 9.1 Ma, $\delta^{13}C_{n\text{-}C29}$ and $\delta^{13}C_{n\text{-}C31}$ values are similar to those of the Early Oligocene, with $\delta^{13}C_{n\text{-}C29}$ and $\delta^{13}C_{n\text{-}C31}$ values becoming ~1‰ and 2–3‰ more positive from 9.1 Ma towards the Present.

3.3. N-alkane hydrogen isotope ratios

The hydrogen isotopic composition of *n*-C_{29} and *n*-C_{31} ($\delta D_{n\text{-}C29}$ and $\delta D_{n\text{-}C31}$, Table 1) are positively correlated ($R^2 = 0.93$). In general, there is a long-term negative trend observed in both $\delta D_{n\text{-}C29}$ and $\delta D_{n\text{-}C31}$

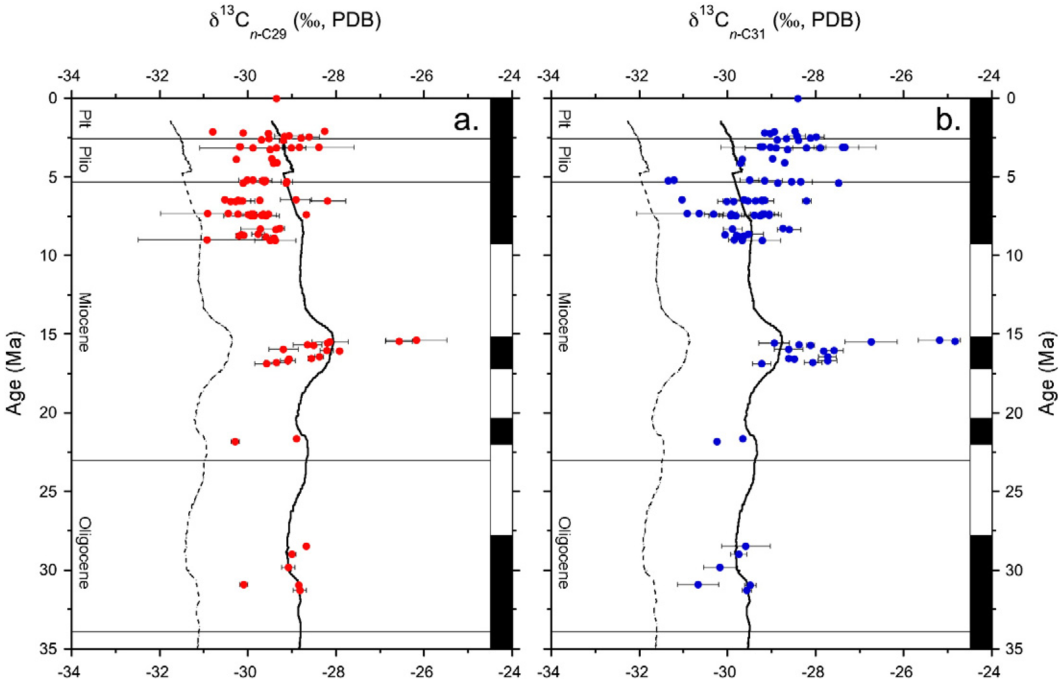

Fig. 3. (a) $\delta^{13}C$ values of *n*-C_{29} *n*-alkanes from Site 94. (b) $\delta^{13}C$ of *n*-C_{31} *n*-alkanes. Black bars represent recovered intervals and white areas are missing material. Black and dotted lines are 1σ and average C_3 end-members $\delta^{13}C$ values for *n*-alkanes. Bars represent the range of duplicate analyses.

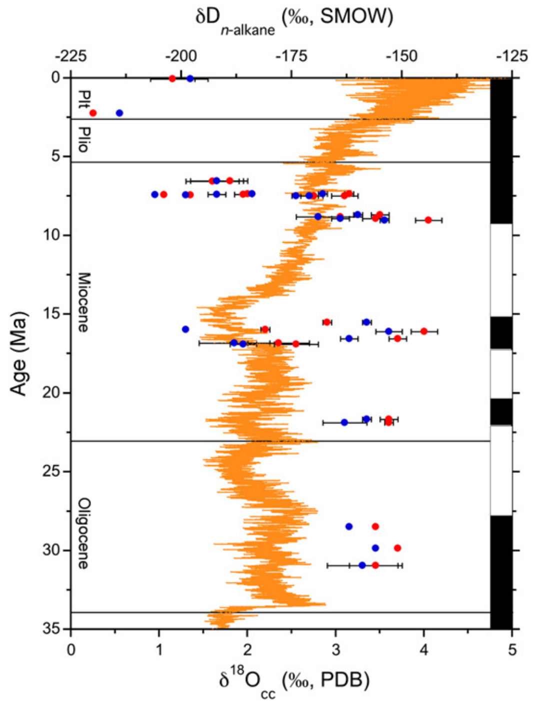

Fig. 4. δD values of *n*-C_{29} and *n*-C_{31} *n*-alkanes from Site 94. Red and blue points represent *n*-C_{29} and *n*-C_{31} δD values, respectively. Error bars represent range of duplicate analyses. Orange line represents benthic foraminifera $\delta^{18}O$ records from Zachos et al. (2001). Black bars represent recovered intervals and white areas are missing material.

from the Oligocene towards the present (Fig. 4), punctuated by rapid changes during the Middle Miocene, and from the Late Miocene to the Pleistocene. $\delta D_{n\text{-}C29}$ and $\delta D_{n\text{-}C31}$ values during the Oligocene–Early Miocene average −155‰ and −165‰, respectively. During the Middle Miocene (16.9–15.4 Ma), both $\delta D_{n\text{-}C29}$ and $\delta D_{n\text{-}C31}$ fluctuate (50‰) (Fig. 4) before $\delta D_{n\text{-}C29}$ and $\delta D_{n\text{-}C31}$ return to baseline values (~−160‰) during the Late Miocene. From 9.0 to 6.5 Ma, $\delta D_{n\text{-}C29}$ and $\delta D_{n\text{-}C31}$ becomes more negative by ~50‰, interrupted by a relatively rapid negative excursion between 7.5 and 7.3 Ma. Pliocene $\delta D_{n\text{-}C29}$ and $\delta D_{n\text{-}C31}$ are 25‰ more negative compared to the latest Miocene $\delta D_{n\text{-}C29}$ and $\delta D_{n\text{-}C31}$ values. Pleistocene $\delta D_{n\text{-}C29}$ and $\delta D_{n\text{-}C31}$ values of ~−200‰ are similar to those in the latest Miocene.

4. Discussion

4.1. Terrestrial higher plant inputs to the Gulf of Mexico, Site 94

The CPI record of Site 94 is consistent with higher plant organic material delivery to the deep regions of the Gulf of Mexico (Table 1, Fig. 2a). While modern higher plant *n*-alkanes have CPI values between 4 and 40, (Bi et al., 2005; Chikaraishi and Naraoka, 2003; Chikaraishi et al., 2004; Collister et al., 1994), *n*-alkanes extracted from modern soils and dust range from 2 to 8 (Huang et al., 1997; Schefuss et al., 2003). Lower sedimentary CPI values likely reflect microbial degradation of higher plant *n*-alkanes (Huang et al., 1997; Schefuss et al., 2003). CPI values alone are not conservative indicators of terrestrial higher plant input as some algae have been shown to produce high molecular weight *n*-alkanes (Lichtfouse et al., 1994). Nonetheless, our CPI values are consistent with Bengal Fan sediment-derived *n*-alkane CPI records of similar age (3.2–6.1; Freeman and Colarusso, 2001) and suggest that the Site 94 Gulf of Mexico high molecular weight *n*-alkanes are predominately from terrestrial plants sourced from the continental interior.

The Mississippi River catchment and delta dominate the terrestrial sedimentary input into the Gulf of Mexico (Hedges and Parker, 1976), contributing organic carbon from various terrestrial environments including material from the continental interior and deltaic margin. Initial studies of Gulf of Mexico sediments, terrestrial plant macrofossils, and lignin concentration provide evidence that terrestrial sources dominate organic material contributions near-shore, suggesting little terrestrial organic carbon is transported to deep, offshore waters (Gearing et al., 1977; Hedges and Parker, 1976). Recent compound-specific isotopic studies and biomarker analysis show a high abundance of terrestrial organic material is associated with fine grain sediments delivered offshore to the outer shelf and slope regions (Goni et al., 1998; Waterson and Canuel, 2008). Isotopic ratios and abundance data of lignin biomarker from Gulf of Mexico surface sediments indicate 40–90% C_4 organic material inputs, suggesting terrestrial organic matter on the outer shelf and slope derives from vegetation of the continental interior, and not from the higher plants of the delta (Goni et al., 1998). Further, these lignin biomarkers have old radiocarbon ages and were likely sourced from soils of the Mississippi River watershed (Goni et al., 1998). Terrestrial leaf waxes can be 5000 years older than the sediment age (Smittenberg et al., 2004), suggesting that *n*-alkanes are well suited for studying longer time intervals.

The Gulf of Mexico receives continental runoff from North American continental interior, the eastern Mexican isthmus, and the Yucatan Peninsula. The Sierra Madre Oriental and Sierra Madre de Guatemala Mountains bisect the Mexican isthmus along the eastern edge and have been a topographical high since the Middle Cretaceous (Alzaga-Ruiz et al., 2009; Ortega-Gutierrez et al., 1994). The Yucatan Peninsula is dominated by karst topography with no major rivers flowing into the Gulf of Mexico. Modern discharge from the Mexican isthmus is an order of magnitude smaller than rivers draining the North American continental interior (Revenga et al., 1998), thus, while some component of higher plant *n*-alkanes derive from eastern Mexico, it is likely a minor contribution compared to the North American continental interior.

In addition to riverine delivery, higher plant *n*-alkanes can be transported by winds into marine settings (Huang et al., 2001; Schefuss et al., 2003; Simoneit, 1997). Today, easterly winds from the southern Sahara and Sahel regions are occasionally present during the summer months and are responsible dust influx to the Gulf of Mexico region (Colarco et al., 2003). It is probable some fraction of terrestrial higher plant *n*-alkanes in Gulf of Mexico sediments derive from Northern Africa. However, African eolian dust records since the Miocene/Pliocene boundary track orbitally modulated high-amplitude variations, with no net increase in dust concentration prior to the Pleistocene (deMenocal, 2004). Consequently, variations in Gulf of Mexico records are likely tracking regional ecosystems and climates, and not African climate and eolian transport. In addition, atmospheric circulation patterns prior to 4.3 Ma with the Intertropical Convergence Zone near ~10°N would preclude sizable dust inputs from Africa into the Gulf of Mexico region via a low-level jet (Gussone et al., 2004).

4.2. Estimates of North American C_4 plant input during the Cenozoic

The stable carbon isotopic composition of higher plants is predominately a function of the carbon isotope composition of the atmospheric CO_2 ($\delta^{13}C_{CO2}$) and the plant's specific photosynthetic pathway (Farquhar et al., 1989), with environmental conditions exerting a minimal influence. Estimates of C_4 plant abundances require knowledge of the average carbon isotope fractionation between atmospheric CO_2 gas and plant organic carbon (ε) for different plant types. Modern ε values for C_3 and C_4 plant *n*-C_{29} $\varepsilon_{CO2\text{–}C29}$ are −25.5 ± 2.6‰ (1σ, n = 320) and −13.5 ± 2.4‰ (1σ, n = 58), while $\varepsilon_{CO2\text{–}C31}$ of C_3 and C_4 plants are −26.1 ± 2.7‰ (1σ, n = 244) and −13.7 ± 2.2‰ (1σ, n = 58), respectively (Fig. 5) (Bi et al.,

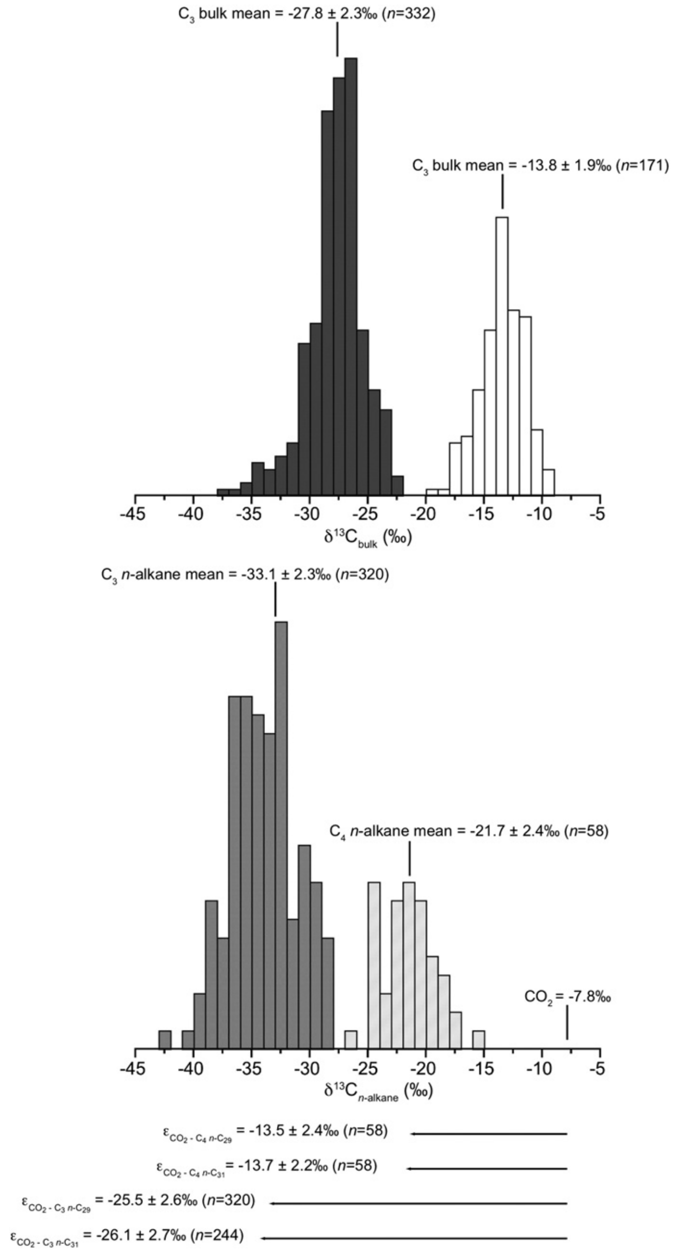

Fig. 5. Histogram of bulk leaf and n-alkane δ^{13}C values. Apparent fractionation between n-C$_{29}$ and n-C$_{31}$ and CO$_2$ for C$_3$ and C$_4$ plants is shown. Data compiled from Cerling et al. (1997), Deines (1980), Bi et al. (2005), Chikaraishi and Naraoka (2003), Chikaraishi et al. (2004), Collister et al. (1994), Lockheart et al. (1997), Rommerskirchen et al. (2006), and Vogts et al. (2009).

2005; Chikaraishi and Naraoka, 2003; Chikaraishi et al., 2004; Collister et al., 1994; Lockheart et al., 1997; Rommerskirchen et al., 2006; Vogts et al., 2009). Proxy records of $\delta^{13}C_{CO2}$ values indicate that $\delta^{13}C_{CO2}$, and by extension, C$_3$ and C$_4$ isotopic end-members varied over the last 35 million years (Tipple et al., 2010). In order to determine the relative contribution of C$_4$ plants through time, we use a reconstructed record of $\delta^{13}C_{CO2}$ from benthic foraminifera (Tipple et al., 2010) in conjunction with modern values of $\varepsilon_{CO2-C29}$ and $\varepsilon_{CO2-C31}$ (Fig. 5), and our $\delta^{13}C_{n\text{-alkanes}}$ records (Fig. 3) to estimate the carbon isotopic end-members of C$_3$ and C$_4$ plants. Changes in the plant sources contributing n-alkanes to the Gulf of Mexico can be examined using an isotopic mixing model:

$$\delta^{13}C_{alk} = \varepsilon_{CO_2-C_3alk} \times f_{C_3alk} + \varepsilon_{CO_2-C_4alk} \times f_{C_4alk} \quad (4)$$

where $\varepsilon_{CO2-C3alk}$ and $\varepsilon_{CO2-C4alk}$ reflect the average isotopic difference between ancient atmospheric CO$_2$ and C$_3$ and C$_4$ n-alkanes, respectively. Variables f_{C3} and f_{C4} are the fractions of each photosynthetic type delivered to Site 94. We model C$_4$ plant percentages assuming Cenozoic C$_3$ and C$_4$ plants maintained an $\varepsilon_{CO2-C29}$ of −25.5‰ and −13.5‰ and $\varepsilon_{CO2-C31}$ of −26.1‰ and −13.7‰ (Fig. 3a and b). Application of average isotopic end-members, suggests 14–23% C$_4$ input to the Gulf of Mexico during the Oligocene and Early Miocene (Fig. 6). C$_4$ influences increase during the warmth of the Middle Miocene with evidence for 18–43% between 15.3 and 16.3 Ma based on $\delta^{13}C_{n\text{-C31}}$ and $\delta^{13}C_{n\text{-C29}}$ records (Fig. 6). During the Late Miocene to Pliocene, $\delta^{13}C_{n\text{-C31}}$ and $\delta^{13}C_{n\text{-C29}}$ values suggest a gradual increase of C$_4$ input into the Gulf of Mexico from 13% to 28%. These estimates should be viewed as maximum estimates as they are likely amplified due to the use of average $\varepsilon_{CO2-C29}$ and $\varepsilon_{CO2-C31}$ values, rather than more conservative end-member estimates.

From ~4 Ma to the Present, average carbon chain length of plant waxes (AHPCL) increased (Fig. 2b) — changes associated with higher growth temperatures, increased aridity, and/or photosynthetic pathway (Hughen et al., 2004; Rommerskirchen et al., 2006; Schefuss et al., 2003; Vogts et al., 2009). We propose that higher AHPCL primarily resulted from a combination of increased C$_4$ plant contribution and aridity within continental North America during the Pliocene.

The evolution of terrestrial plant ecosystems of the Great Plains have been evaluated from δ^{13}C records of herbivore tooth enamel and soil carbonates (Cerling et al., 1997; Fox and Koch, 2003, 2004; Passey et al., 2002). In general, these records support C$_4$-grassland expansion during the late Miocene/Pliocene (Fig. 6). Tooth enamel records indicate a rapid shift in C$_4$-plant contribution to equid diets (Cerling et al., 1997; Passey et al., 2002), while soil carbonates show a more gradual change in grassland ecosystems (Fox and Koch, 2003, 2004). Importantly, herbivore tooth enamel and soil carbonates δ^{13}C records track different processes of the terrestrial environment. Herbivore tooth enamel carbon isotope ($\delta^{13}C_{enamel}$) records are repositories of diet information and the general absence/presence of C$_4$ graze on the landscape. Assuming specific soil conditions, soil carbonate δ^{13}C values ($\delta^{13}C_{SC}$) reflect a seasonally weighted record of plant community. Given that large herbivores can travel great distances, $\delta^{13}C_{enamel}$ records provide a regional-scale isotope signal of diet. In contrast, paleosol carbonate $\delta^{13}C_{SC}$ records are inherently site-specific. $\delta^{13}C_{SC}$ records are not biased toward a particular plant type,

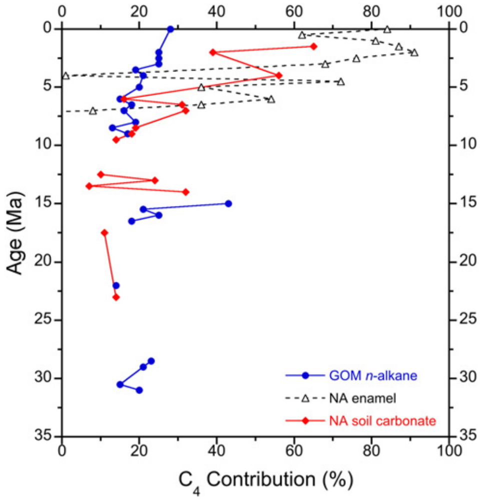

Fig. 6. Mixing model of C$_4$ material delivered to marine sediments. Blue dots show estimates of C$_4$ plant input over the last 35 Myr using average n-alkane δ^{13}C values. Black triangles and red diamonds are estimates of C$_4$ plant from North American tooth enamel and soil carbonate δ^{13}C records binned into 0.5 Myr data windows (Cerling et al. 1997; Fox and Koch, 2003; Passey et al., 2002).

unlike enamel records owing to feeding selectivity, and thus provide a more integrated isotope signal of the actual plant community. As a result, enamel $\delta^{13}C_{enamel}$ values show a distinct change from C_3 to C_4-dominated diets between 8 and 4 Ma, while soil carbonate $\delta^{13}C$ records from the North American Great Plains provide compelling evidence that C_4 plants made up a sizable component (>20%) of the plant community throughout much of the Miocene (Fox and Koch, 2003, 2004).

Differences between terrestrial-based and marine-based proxies are anticipated because tooth enamel and soil records are weighted towards grassland systems (Cerling et al., 1997), whereas the sediments in the Gulf of Mexico reflect the character of the entire drainage. When previously established North American carbon isotope records are assessed in relationship to changes in $\delta^{13}C_{CO2}$, binned into 0.5 Myr data windows, and compared to our *n*-alkane records, we find distinct similarities in regard to C_4 plant input in relationship to our record (Fig. 6). However, our records show distinct differences during the Mid-Miocene and suggest up to 43% C_4 contribution while the other proxies indicate only modest increases.

Increased diversification of the C_4 pathway in several C_4 clades has been implicated during the middle Miocene (Christin et al., 2008; Vincentini et al., 2008). Given that an increase in C_4 contribution is not observed in Great Plains terrestrial isotope records, enhanced C_4 plant delivery observed in our record could reflect a signal endemic to North America resulting from a broader sampling terrestrial environments or an enhanced contribution of eolian materials from the African continent. In either case, our data support a sizable contribution of C_4 plant materials from North America during the Middle Miocene that is not recorded elsewhere.

4.3. N-alkane hydrogen isotopic compositions and relationship to Cenozoic climate

Water delivery to the central North America and the Mississippi River watershed is strongly seasonal with the dominant moisture pathways originating from three distinct air-mass source regions — the Atlantic Ocean and Gulf of Mexico, the Pacific Ocean, and the Arctic (Bryson and Hare, 1974). The isotopic composition of precipitation and river water reflects these seasonal source differences, with Gulf of Mexico moisture substantially D-enriched compared to the Pacific source (International Atomic Energy Agency, 2001; Kendall and Coplen, 2001). Seasonally averaged Mississippi catchment precipitation and river δD values range from −20‰ in Louisiana to −140‰ in Southern Alberta (International Atomic Energy Agency, 2001; Kendall and Coplen, 2001), while the δD of the Great Plain grass *n*-alkanes range from −235‰ in North Dakota to −208‰ in Central Kansas (Smith and Freeman, 2006).

Seasonal precipitation maxima for much of the central and northern Great Plains occur during the spring (Mock, 1996) associated with a long wave trough that develops over the west central United States moving west to east. This trough brings Pacific moisture to the northern Plains (Harman, 1991), while a low-level jet transports warm moist air from the Gulf of Mexico to the southern and coastal Plains (Helfand and Schubert, 1995). Typically, late summer precipitation decreases in the Plains, but some areas in the central and southern Great Plain have secondary precipitation maxima in September related to trajectories of Atlantic/Gulf of Mexico tropical storms (Harman, 1991; Keables, 1989). Winter precipitation amounts in the Plains are low, with the northern and central Plains receiving moisture from the Pacific Ocean with minor contributions from the Arctic region, and the southern Plains receiving moisture from the Gulf of Mexico.

We recognize our low-resolution records limit interpretations to only a broad summary of long-term trends (Fig. 4). However, clear patterns emerge from absolute isotopic values and variations. For example, comparatively little isotopic variability is apparent from the Oligocene to the Early Miocene, suggesting little change in moisture source or aridity in central North America (Fig. 4) — an observation consistent with other continental estimates of precipitation (Fox and Koch, 2004; Passey et al., 2002).

Middle Miocene hydrogen isotope records (δD_{alk}) show higher variability ranging between −141 and −200‰ over ~1.5 million years (Fig. 4), reflecting increased variability in plant communities and the regional hydrological cycle as global temperatures reached a climatic optimum near 14 Ma (Flowers and Kennett, 1994). This interpretation is consistent with results from continental paleosols and macrofossils from North America that indicate increases in precipitation (Retallack, 2007) and temperature and/or evaporation (Fox and Koch, 2004; Retallack, 2007), as well as an expansion of thermophilic plant taxa (Wolfe, 1994) during this time.

Evapotranspiration and a plant's specific water-use efficiency influence the δD value of modern leaf waxes (Hou et al., 2008). We anticipate that relatively minor changes in the rates of evaporation or the composition of plant communities would alter the character of δD_{alk}. Indeed, across intervals where C_4 plant contributions are inferred to increase, δD_{alk} becomes increasingly positive (Fig. 4). However, by the end of the Middle Miocene when global temperatures and $\delta^{13}C$ values indicates that C_4 contributions reached their maximum (Fig. 4), δD_{alk} is comparatively more D-depleted, suggesting either a relaxation of evaporative conditions, changes in source region and moisture pathways or plant community variation (Fig. 4).

If C_3 grasses were replaced by C_4 grasses during the Late Miocene into the Pliocene, as suggested by phytolith data (Strömberg, 2005), sedimentary δD_{alk} values are predicted to become more D-enriched due to differences in $\varepsilon_{alk-water}$. In contrast to this expectation, δD_{alk} values become ~75‰ more negative from the Late Miocene toward the Pliocene (Fig. 4). If our isotope record reflects C_4 expansion in the Great Plains, then ecological change could have primarily occurred at the expense of C_3 trees and other dicots instead of C_3 grasses, resulting in a maximum negative δD_{alk} shift of only ~20‰. Thus other hydrological/climatic factors must have contributed to the isotopic changes reflected in the long-term δD_{alk}, or regional-scale plant community variations are more complex than suggested by phytolith data.

The influences of plant community and hydrologic conditions can be decoupled by exploring relationships between both $\delta^{13}C_{alk}$ and δD_{alk} values in consideration of isotopic ranges expressed by C_3 dicots, C_3 monocots and C_4 monocots. C_3 and C_4 plants have average $\varepsilon_{CO2-C31}$ values of −26.1‰ and −13.7‰, respectively. The average C_3 dicot has an approximate $\varepsilon_{lipid-water}$ value of −110‰, while C_3 monocots and C_4 monocots have $\varepsilon_{lipid-water}$ values of −165‰ and 140‰, respectively (Chikaraishi and Naraoka, 2003; Feakins and Sessions, 2010; Sachse et al., 2006, 2009; Smith and Freeman, 2006). If the isotopic composition of CO_2 and source water is reasonably constrained then a triangular zone of plant community $\delta^{13}C/\delta D$ solutions can be described (Fig. 7). Data that falls outside the boundaries of these isotopic fields arguably require hydrological changes in their interpretation.

Here we use $\delta^{13}C_{CO2}$ proxy records (Tipple et al., 2010) to describe C_3 and C_4 isotopic end-members and assume C_3 trees dominated the Oligocene North American landscape within the Mississippi watershed (Strömberg, 2005). To assess if the δD of source water varied over the last 35 Myr, we define Oligocene source water δD as −45‰ using the measured δD_{alk} and $\varepsilon_{lipid-water}$ for C_3 dicots to solve for source water δD. A modern mean-annual precipitation value of −45‰ corresponds to a broad region of the lower Mississippi watershed from Texas to Indiana.

We find little variability in Oligocene and Early Miocene plant communities that were dominated by C_3 dicots (Fig. 7), in line with other proxies of plant community dynamics (Strömberg, 2005). During the Middle Miocene, a shift towards more mixed communities of C_3 trees, C_3 grasses, and C_4 grasses can be invoked, followed by a return to more C_3 dicot-dominated communities from 9.1 to 7.5 Ma

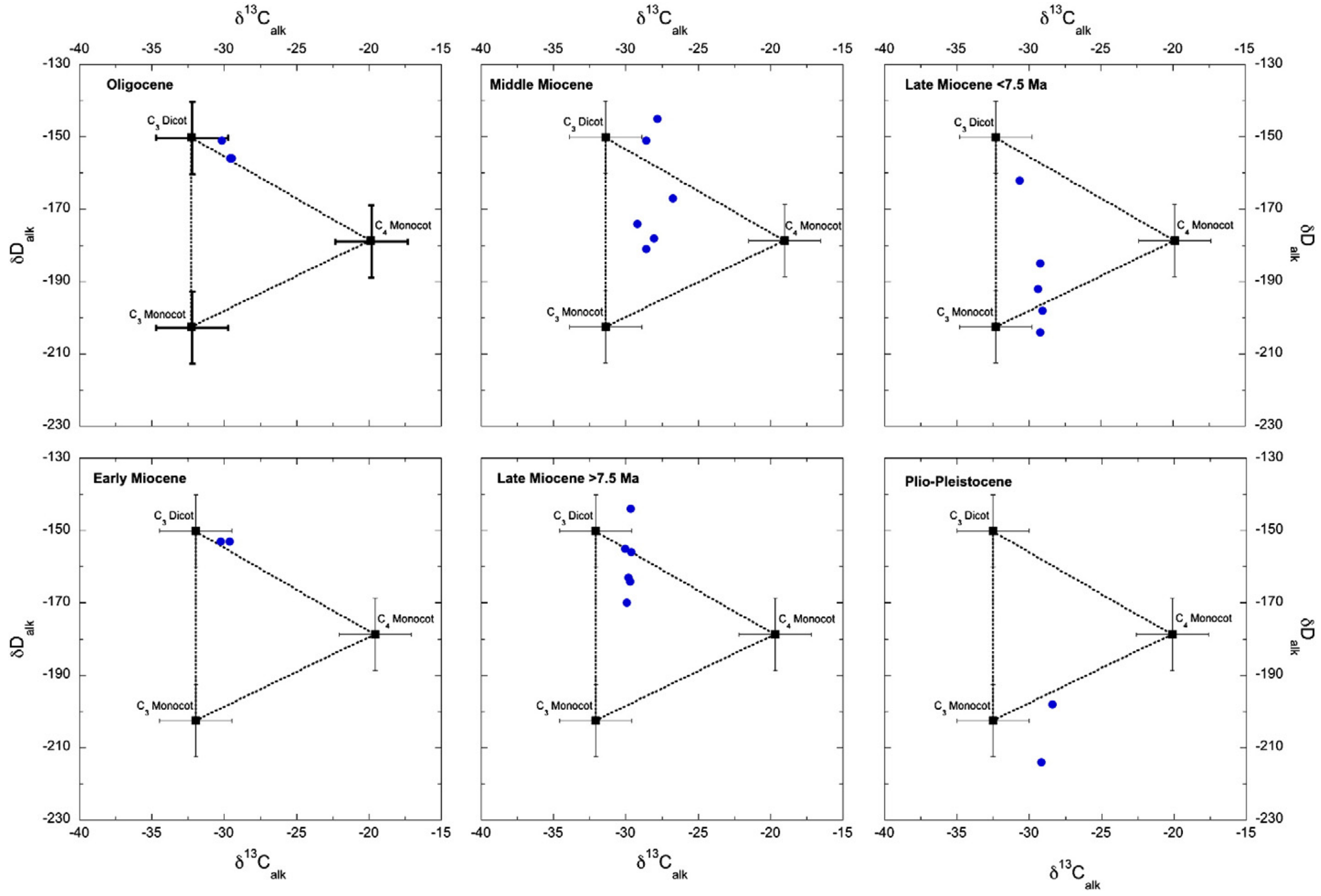

Fig. 7. Cross-plots of *n*-C_{31} δD and $\delta^{13}C$ values from six time intervals. Black squares correspond to end-member δD and $\delta^{13}C$ values of C_3 dicots, C_3 monocots, and C_4 monocots. $\delta^{13}C$ end-member values for C_3 and C_4 plants were defined using the average $\delta^{13}C_{CO2}$ value for each time interval from Tipple et al. (2010). δD end-members assigned using a precipitation δD value of −45‰ as described in the text. Error bars represent ±2.7‰ and ±10‰ for carbon and hydrogen isotope ratios, respectively.

(Fig. 7). After 7.5 Ma to the end of the Miocene, $\delta^{13}C$/δD values are consistent with a mixed C_3 and C_4 grass ecosystem. This model suggests that after 7.5 Ma the regional plant community shifted to a grass dominated ecosystem at the expense of trees.

In sum, the Oligocene to the Late Miocene $\delta^{13}C$/δD values are consistent with a relatively stable precipitation δD value as all measured $\delta^{13}C_{alk}$ and δD_{alk} data remain within end-member constraints and uncertainty. We observe one data point that falls well outside the end-member constraints during the Pliocene (Fig. 7), suggesting plant community variation cannot account for the measure $\delta^{13}C$/δD values and requires a change in source water δD value to resolve the data. While the δD end-member values and starting precipitation δD_{alk} value used in this example are ultimately unconstrained, this model effectively demonstrates how variations in δD records can be explained by both variations in plant communities and/or hydrology.

Several scenarios could explain the δD_{alk} value from the Pliocene including (1) a decrease in evapotranspiration, (2) phase change from vapor to precipitation at cooler temperatures, (3) a substantial change in the source of terrestrial material, or (4) changes in the regional hydrologic cycle.

Evaporative stress are positively related to δD values of terrestrial plants (Feakins and Sessions, 2010; Hou et al., 2008). However, the evaporative conditions likely increased during the Pliocene (Rea, 1994). In addition, the Pliocene was a period of global cooling (Zachos et al., 2001) and thermodynamics predicts lower δD values of precipitation associated with lower temperatures of formation (Majoube, 1971), with a decrease of ~10 °C to account for the observed changes in δD. Global cooling cannot be ruled out as a partial contributor to the observed changes in δD_{alk} values.

The Late Miocene/Pliocene reflects a transitional period from relatively warm global temperatures of the Late Miocene to the onset of the Northern Hemisphere glaciations of the Late Pliocene (Zachos et al., 2001). Hemispheric hydrological cycles likely responded, and perhaps contributed to, global climate change during the late Tertiary (Driscoll and Haug, 1998). The closure of the Panamanian Seaway has been argued as an important step in the development of Late Miocene/Pliocene climate by altering global heat transport and impacting thermohaline circulation (Haug and Tiedemann, 1998). Low latitude warm surface waters were likely redirected northward, introducing a new moisture source for Northern Hemisphere glaciation (Driscoll and Haug, 1998; Duque-Caro, 1990). Northern Hemisphere cooling led to an increase meridional wind strength and heat transport (Chaisson and Ravelo, 2000; Vellinga and Wood, 2002), as indicated by increased dust flux and inferred wind strength (Rea, 1994). Changes in hemispheric moisture and pressure systems would have potentially altered the source regions of terrestrial lipids reaching the Gulf of Mexico, as well as the source regions of precipitation. For example, it is possible that prior to the Late Miocene, sediments delivered to Site 94 were weighted towards plant material from the tropics. Increased incision rates in the Rocky Mountains from 17.5 to 5.0 Ma (McMillan et al., 2002, 2006) support increased sediment delivery to the Mississippi catchment during the terminal Miocene with global incision rates and sediment fluxes accelerating coincident with the global cooling trend beginning at

~3 Ma (Zhang et al., 2001). However, if a change in sediment provenance and delivery was driving isotope signals in the Gulf of Mexico, we would expect to see a change in δD_{alk} values during the Early Miocene and not the latest Miocene and Pliocene as observed (Fig. 6). Ultimately, effects specific to the hydrologic cycle need to be considered to explain our isotope record (Fig. 6). One probable explanation involves linkages between the hydrologic cycle and tectonics. For example, the shoaling of the Panamanian Seaway during the latest Miocene (Duque-Caro, 1990), arguably shifted the position of the Intertropical Convergence Zone (ITCZ) from 10°N to its present latitude; ~0°N (Billups et al., 1999; Gussone et al., 2004). This shift in the ITCZ likely positioned Northern Hemisphere pressure systems to locations more southerly and more similar to modern atmospheric patterns (Gussone et al., 2004). Further, the early Pliocene (5–3 Ma) climate of North America was influenced by the establishment of a permanent El Niño (Fedorov et al., 2005; Molar and Cane, 2007). Today, El Niño years are characterized by increased summer precipitation and decreased temperatures in southern Great Plains and coastal plain while the northern Great Plain and southwest have increased summer temperatures and precipitation. Increased summer precipitation in the Great Plains is due to convergence between northerly flow from the Pacific Ocean associated with the warm northeastern Pacific and southerly flow originating from the Gulf of Mexico associated with the warming of the tropical central-eastern Pacific Ocean (Yang et al., 2007). Numerous studies of Late Miocene and Early Pliocene lake sediments suggest that hydrological conditions were consistent with an El Niño state, with wet climates in the northern, central, and southern Great Plains (Forester, 1991; Shunk et al., 2006, 2009; Smith, 1994; Smith and Patterson, 1994; Smith et al., 1993; Thompson, 1991). We suggest that the southward shift in the ITCZ and increased meridional wind strength led to the development of a modern Pacific high-pressure system, transporting more Pacific moisture into the Mississippi watershed — amplified during the summer months by the permanent El Niño conditions. Thus, the trend toward more negative δD_{alk} values during the Pliocene was promoted by precipitation increasingly characterized as a mixture of Pacific and Gulf of Mexico sources. The establishment of a bimodal hydrological system of Pacific and Gulf of Mexico sources implies seasonal Pacific moisture delivery during the spring and fall — enhancing a seasonal precipitation pattern that favored C_4 plant growth.

Others have suggested that the southeastern North American monsoon was established during the Late Miocene and early Pliocene (Shunk et al., 2009). Prior to the closure of the Panamanian Seaway and the presence of a warm Gulf Stream, cool Atlantic surface waters were associated with the southeastern North American coast (Haug and Tiedemann, 1998; Maier-Reimer et al., 1990). Late Miocene and Early Pliocene marine and terrestrial paleoclimate records suggest highly-productive, cooler surface waters (Snyder et al., 2001) and the development of stronger temperature and pressure gradients between the continent and ocean relative to today (Shunk et al., 2009). Presently, the southeastern coastal plain experiences monsoonal precipitation during the summer months. During the Late Miocene, lower coastal sea surface temperatures would have potentially promoted a stronger monsoonal system (Shunk et al., 2009). If so, a moist summer growing season with relatively D-enriched precipitation would have also favored C_4 plant ecosystems.

5. Conclusion

We measured $\delta^{13}C$, δD and compound distributions of higher plant *n*-alkanes from Gulf of Mexico sediments (DSDP Site 94) in order to assess the relationship between Cenozoic North American climate and C_4 grass expansion. Sedimentary *n*-alkane distributions reflect higher plants sourced predominately from the vast Mississippi watershed. Estimates for the proportion of C_4 plant delivery was modeled by considering changes in the $\delta^{13}C$ of atmospheric CO_2. Our data are consistent with the interpretation of little to no C_4 plant input prior to the Early Miocene, a clear increase during the Middle Miocene Climatic Optimum, and greater C_4 plant delivery from the Late Miocene into the Pliocene to the Present.

Taken together, the $\delta^{13}C$, δD, and compound distributions suggest a dynamic interaction between regional and global forces driving expansion of C_4 grassland in North America. While low CO_2 was likely a precondition for the development of C_4 grasses, this study indicates that gross plant community change alone can account for the observed shifts in plant δD values from the Oligocene to the Miocene, and that changes in regional hydrology potentially influenced C_4 grassland expansion during the Pliocene. We interpret our isotope records to reflect changes both moisture source regions and in seasonality of precipitation associated with the shoaling of the Panamanian Seaway.

Acknowledgements

We are grateful to M. Hren and D. Zinniker for their input. In addition, we would like to thank K. Metzger and A. Veach for their efforts in the laboratory. All isotope analyses were performed at the Yale Institute for Biospheric Studies–Earth Systems Center for Stable Isotopic Studies. This research was supported by grants from the American Chemical Society: PRF grant #39552-AC2, Global Contributions of C4 Plants to Terrestrial Photosynthesis during the Cenozoic awarded to MP, and a NSF-Graduate Research Fund awarded to BT. Jay Quade, Sarah Feakins, and three anonymous referees provided very constructive reviews that greatly improved this manuscript.

References

Alzaga-Ruiz, H., Lopez, M., Roure, F., Seranne, M., 2009. Interactions between the Laramide Foreland and the passive margin of the Gulf of Mexico: tectonics and sedimentation in the Golden Lane area, Veracruz State, Mexico. Mar. Petrol. Geol. 26, 951–973.

Berggren, W.A., Kent, D.V., Swisher, C.C.I., Aubry, M.-P., 1995. A revised Cenozoic geochronology and chronostratigraphy. In: Berggren, W.A., Kent, D.V., Aubry, M.-P., Hardenbol, J. (Eds.), Geochronology Time Scales and Global Stratigraphic Correlation. Society for Sedimentary Geology, Tulsa, Oklahoma.

Bi, X., Sheng, G., Liu, X., Li, C., Fu, J., 2005. Molecular and carbon and hydrogen isotopic composition of *n*-alkanes in plant leaf waxes. Org. Geochem. 36 (10), 1405–1417.

Billups, K., Ravelo, A.C., Zachos, J.C., Norris, R.D., 1999. Link between oceanic heat transport, thermohaline circulation, and the Intertropical Convergence Zone in the early Pliocene Atlantic. Geology 27, 319–322.

Bouchenak-Khelladi, Y., et al., 2009. The origins and diversification of C_4 grasses and savanna-adapted ungulates. Global Change Biol. 1–21.

Boyce, R.E., 1973. Carbon and carbonate analyses, Leg 10. Initial Reports from Deep Sea Drilling Project Leg 10. Deep Sea Drilling Project, Washington, D.C., pp. 641–642.

Bryson, R.A., Hare, F.K., 1974. Climates of North America. World Survey of Climatology, 11. Elsevier, Amsterdam. 420 pp.

Canfield, D.E., 1997. The geochemistry of river particulates from the continental USA: major elements. Geochim. Cosmochim. Acta 61 (16), 3349–3365.

Cerling, T.E., et al., 1997. Global vegetation change through the Miocene/Pliocene boundary. Nature 389, 153–158.

Chaisson, W.P., Ravelo, A.C., 2000. Pliocene development of the east-west hydrographic gradient in the equatorial Pacific. Paleoceanography 15 (5), 497–505.

Chikaraishi, Y., Naraoka, H., 2003. Compound-specific δD-$\delta^{13}C$ analyses of *n*-alkanes extracted from terrestrial and aquatic plants. Phytochemistry 63, 361–371.

Chikaraishi, Y., Naraoka, H., Poulson, S.R., 2004. Hydrogen and carbon isotopic fractionations of lipid biosynthesis among terrestrial (C_3, C_4 and CAM) and aquatic plants. Phytochemistry 65, 1369–1381.

Christin, P.-A., Salamin, N., Savolainen, V., Duvall, M.R., Besnard, G., 2007. C-4 photosynthesis evolved in grasses via parallel adaptive genetic changes. Curr. Biol. 17, 1241–1247.

Christin, P.-A., Petitpierre, B., Salamin, N., Buchi, L., Besnard, G., 2008. Evolution of C4 phosphoenolpyruvate carboxykinase in grasses, from genotype to phenotype. Mol. Biol. Evol. 26 (2), 357–365.

Colarco, P.R., et al., 2003. Saharan dust transport to the Caribbean during PRIDE: 2. Transport, vertical profiles, and deposition in simulations of in situ and remote sensing observations. J. Geophys. Res. 108, 8590.

Collister, J., Reiley, G., Stern, B., Eglinton, G., Fry, B., 1994. Compound-specific $\delta^{13}C$ analysis of leaf lipids from plants with differing carbon dioxide metabolisms. Org. Geochem. 21, 619–627.

DeConto, R., Pollard, D., 2003. Rapid Cenozoic glaciation of Antarctica induced by declining atmospheric CO_2. Nature 421, 245–249.

Deines, P., 1980. The isotopic composition of reduced organic carbon. In: Fritz, P., Fontes, J.C. (Eds.), Handbook of Environmental Isotope Geochemistry: I. The Terrestrial Environment. Elsevier, Amsterdam, pp. 329–406.

deMenocal, P.B., 2004. African climate change and faunal evolution during the Pliocene–Pleistocene. Earth Planet. Sci. Lett. 220 (1), 3–24.

Dettman, D.L., et al., 2001. Seasonal stable isotope evidence for a strong Asian monsoon throughout the past 10.7 m.y. Geology 29 (1), 31–34.

Dinnel, S., Wiseman Jr., W., 1986. Freshwater on the Louisiana shelf. Cont. Shelf Res. 6, 765–784.

Driscoll, N.W., Haug, G.H., 1998. A short circuit in thermohaline circulation: a cause for northern hemisphere glaciation? Science 282 (5388), 436–438.

Duque-Caro, H., 1990. Neogene stratigraphy, paleoceanography and paleobiogeography in northwest South America and the evolution of the Panama Seaway. Palaeogeogr. Palaeoclimatol. Palaeoecol. 77 (3–4), 203–234.

Edwards, E.J., Osborne, C.P., Stromberg, C.A.E., Smith, S.A., C_4 Grass Consortium, 2010. The origins of C_4 grasslands: integrating evolutionary and ecosystem science. Science 328 (5978), 587–591.

Ehleringer, J.R., Cerling, T.E., Helliker, B.R., 1997. C_4 photosynthesis, atmospheric CO_2, and climate. Oecologia 112, 285–299.

Farquhar, G.D., Ehleringer, J.R., Hubick, K.T., 1989. Carbon isotope discrimination and photosynthesis. Annu. Rev. Plant Physiol. Mol. Biol. 40, 503–537.

Feakins, S.J., Sessions, A.L., 2010. Controls on the D/H ratios of plant leaf waxes from an arid ecosystem. Geochim. Cosmochim. Acta 74 (7), 2128–2141.

Feakins, S.J., deMenocal, P.B., Eglinton, T.I., 2005. Biomarker records of late Neogene changes in northeast Africa vegetation. Geology 33 (12), 977–980.

Feakins, S.J., Eglinton, T.I., deMenocal, P.B., 2007. A comparison of biomarker records of northeast African vegetation from lacustrine and marine sediments (ca. 3.40 Ma). Org. Geochem. 38 (10), 1607–1624.

Fedorov, A.V., et al., 2005. The Pliocene paradox (mechanisms for a permanent El Nino). Science 312 (5779), 1485–1489.

Flowers, B.P., Kennett, J.P., 1994. The middle Miocene climatic transition: East Antarctic ice sheet development, deep ocean circulation and global carbon cycling. Palaeogeogr. Palaeoclimatol. Palaeoecol. 108, 537–555.

Forester, R.M., 1991. Pliocene-climate history of the western United States derived from lacustrine ostracodes. Quatern. Sci. Rev. 10 (2–3), 133–146.

Fox, D.L., Koch, P.L., 2003. Tertiary history of C_4 biomass in the Great Plains, USA. Geology 31 (9), 809–812.

Fox, D.L., Koch, P.L., 2004. Carbon and oxygen isotopic variability in Neogene paleosol carbonates: constraints on the evolution of the C_4-grasslands of the Great Plains, USA. Palaeogeogr. Palaeoclimatol. Palaeoecol. 207, 305–329.

Freeman, K.H., Colarusso, L.A., 2001. Molecular and isotopic records of C_4 grassland expansion in the late Miocene. Geochim. Cosmochim. Acta 65 (9), 1439–1454.

Galloway, W.E., et al., 1991. Cenozoic. In: Salvador, A. (Ed.), The Gulf of Mexico Basin. The Geology of North America. The Geological Society of America, Boulder, CO.

Gearing, P., Plucker, F.E., Parker, P.L., 1977. Organic carbon stable isotope ratios of continental margin sediments. Mar. Chem. 5, 251–266.

Goni, M.A., Ruttenberg, K.C., Eglinton, T.I., 1998. A reassessment of the sources and importance of land derived organic matter in surface sediments from the Gulf of Mexico. Geochim. Cosmochim. Acta 62, 3055–3075.

Gussone, N., et al., 2004. Reconstruction of Caribbean Sea surface temperature and salinity fluctuations in response to the Pliocene closure of the Central American Gateway and radiative forcing, using $\delta^{44/40}$Ca, δ^{18}O and Mg/Ca ratios. Earth Planet. Sci. Lett. 227, 201–214.

Harman, J.R., 1991. Synoptic climatology of the westerlies: process and patterns. Resource Publications for College Geography. Association of American Geographers, Washington, D.C. 80 pp.

Haug, G.H., Tiedemann, R., 1998. Effect of the formation of the Isthmus of Panama on Atlantic Ocean thermohaline circulation. Nature 393 (6686), 673–676.

Hay, W.W., 1973. Preliminary dating by fossil calcareous nannoplankton, Deep Sea Drilling Project-Leg 10. Initial Reports of the Deep Sea Drilling Project, Leg 10. Deep Sea Drilling Project, Washington, D.C.

Hedges, J.I., Parker, P.L., 1976. Land-derived organic matter in surface sediments from the Gulf of Mexico. Geochim. Cosmochim. Acta 40, 1019–1029.

Helfand, H.M., Schubert, S.D., 1995. Climatology of the simulated great-plains low-level jet and its contribution to the continental moisture budget of the United States. J. Climate 10 (4), 784–806.

Hou, J., Huang, Y., Oswald, W.W., Foster, D.R., Shuman, B., 2007. Centennial-scale compound-specific hydrogen isotope record of Pleistocene–Holocene climate transition from southern New England. Geophys. Res. Lett. 34, L19706.

Hou, J., D'Andrea, W.J., Huang, Y., 2008. Can sedimentary leaf waxes record D/H ratios of continental precipitation? Field, model, and experimental assessments. Geochim. Cosmochim. Acta 72, 3503–3517.

Huang, Y., et al., 1997. Absence of carbon isotope fractionation of individual *n*-alkanes in a 23 year field decomposition experiment with *Calluna vulgaris*. Org. Geochem. 26, 497–501.

Huang, Y., et al., 2001. Climate change as the dominant control on glacial–interglacial variations in C_3 and C_4 plant abundance. Science 293 (5535), 1647–1651.

Huang, Y., Clemens, S.C., Liu, W., Wang, Y., Prell, W.L., 2007. Large-scale hydrological change drove the late Miocene C_4 plant expansion in the Himalayan foreland and Arabian Peninsula. Geology 35 (6), 531–534.

Hughen, K.A., Eglinton, T.I., Xu, L., Makou, M., 2004. Abrupt tropical vegetation response to rapid climate changes. Science 304, 1955–1959.

International Atomic Energy Agency, 2001. GNIP Maps and Animations. International Atomic Energy Agency, Vienna.

Jacobs, B.F., Kingston, J.D., Jacobs, L.L., 1999. The origin of grass-dominated ecosystems. Ann. Missouri Bot. Gard. 86, 590–643.

Janis, C.M., Damuth, J., Theodor, J.M., 2000. Miocene ungulates and terrestrial primary productivity: where have all the browsers gone? Proc. Natl Acad. Sci. U. S. A. 97 (4), 7899–7904.

Keables, M.J., 1989. A synoptic climatology of the bimodal precipitation distribution in the upper Midwest. J. Climate 2 (11), 1289–1294.

Keeley, J.E., Rundel, P.W., 2005. Fire and the Miocene expansion of C_4 grasslands. Ecol. Lett. 8, 683–690.

Kellogg, E.A., 2001. Evolutionary history of the grasses. Plant Physiol. 125, 1198–1205.

Kendall, C., Coplen, T.B., 2001. Distribution of oxygen-18 and deuterium in river waters across the United States. Hydrol. Process. 15, 1363–1393.

Kiatta, H.W., 1971. The stratigraphy and petroleum potential of the lower Miocene, offshore Galveston and Jefferson Counties, Texas. Gulf Coast Assoc. Geol. Soc. Trans. 21, 257–270.

Koch, P.L., 1998. Isotopic reconstruction of past continental environments. Annu. Rev. Earth Planet. Sci. 26, 573–613.

Kurschner, W.M., Kvacek, Z., Dilcher, D.L., 2008. The impact of Miocene atmospheric carbon dioxide fluctuations on climate and the evolution of terrestrial ecosystems. Proc. Natl Acad. Sci. U. S. A. 105, 449–453.

Latorre, C., Quade, J., McIntosh, W.C., 1997. The expansion of C_4 grasses and global change in the late Miocene: stable isotope evidence from the Americas. Earth Planet. Sci. Lett. 146 (1), 83–96.

Lawver, L.A., Gahagan, L.M., 2003. Evolution of Cenozoic seaways in the circum-Antarctic region. Palaeogeogr. Palaeoclimatol. Palaeoecol. 198 (1), 11–37.

Lichtfouse, E., Derenne, S., Mariotti, A., Largeau, C., 1994. Possible algal origin of long chain odd *n*-alkanes in immature sediments as revealed by distributions and carbon isotope ratios. Org. Geochem. 22, 1023–1027.

Lockheart, M.J., Van Bergen, P.F., Evershed, R.P., 1997. Variation in the stable carbon isotope composition of individual lipids from the leaves of modern angiosperms: implications for the study of higher land plant-derived sedimentary organic matter. Org. Geochem. 26, 137–153.

Lowenstein, T.K., Demicco, R.V., 2006. Elevated Eocene atmospheric CO_2 and its subsequent decline. Science 313 (5795), 1928.

MacGinitie, H.D., 1962. The Kilgore flora; a Late Miocene flora from Northern Nebraska. Univ. Calif. Publ. Geol. Sci. 35, 67–158.

Maier-Reimer, E., Mikolajewicz, U., Crowley, T., 1990. Ocean general circulation model sensitivity experiment with an open Central American Isthmus. Paleoceanography 5 (3), 349–366.

Majoube, M., 1971. Fractionnement en oxygen et en deuterium entre l'eau et sa vapeur. J. Chim. Phys. 68, 1423–1436.

Marzi, R., Torkelson, B.E., Olson, R.K., 1993. A revised carbon preference index. Org. Geochem. 20, 1303–1306.

McMillan, M.E., Angevine, C.L., Heller, P.L., 2002. Postdepositional tilt of the Miocene-Pliocene Ogallala Group on the western Great Plains: evidence of late Cenozoic uplift of the Rocky Mountains. Geology 30 (1), 63–66.

McMillan, M.E., Heller, P.L., Wing, S.L., 2006. History and causes of post-Laramide relief in the Rocky Mountain orogenic plateau. Geol. Soc. Am. Bull. 118 (3/4), 393–405.

Mock, C.J., 1996. Climatic Controls and spatial variations of precipitation in the western United States. J. Climate 9 (5), 1111–1125.

Molar, P., Cane, M.A., 2007. Early Pliocene (pre–Ice Age) El Niño–like global climate: which El Niño? Geosphere 3 (5), 337–365.

Ortega-Gutierrez, F., Sedlock, R.L., Speed, R.C., 1994. Phanerozoic tectonic evolution of Mexico. In: Speed, R.C. (Ed.), Phanerozoic Evolution of North American Continent-Ocean Transitions, pp. 265–306.

Osborne, C.P., 2008. Atmosphere, ecology and evolution: what drove the Miocene expansion of C_4 grasslands? J. Ecol. 96 (1), 35–45.

Osborne, C.P., Beerling, D.J., 2006. Nature's green revolution: the remarkable evolutionary rise of C_4 plants. Philos. Trans. R. Soc. Lond. B Biol. Sci. 361 (1465), 173–194.

Pagani, M., Freeman, K.H., Arthur, M.A., 1999. Late Miocene atmospheric CO_2 concentrations and the expansion of C_4 grasses. Science 285 (5429), 876–879.

Pagani, M., Zachos, J.C., Freeman, K.H., Tipple, B.J., Bohaty, S., 2005. Marked decline in atmospheric carbon dioxide concentrations during the Paleogene. Science 309, 600–603.

Passey, B.H., et al., 2002. Environmental change in the Great Plains: an isotopic record from fossil horses. J. Geol. 110, 123–140.

Pearson, P.N., Palmer, M.R., 2000. Atmospheric carbon dioxide concentrations over the past 60 million years. Nature 406, 695–699.

Pedentchouk, N., Sumner, W., Tipple, B.J., Pagani, M., 2008. δ^{13}C and δD compositions of *n*-alkanes from modern angiosperms and conifers: an experimental set up in central Washington State, USA. Org. Geochem. 39 (8), 1066–1071.

Quade, J., Cerling, T.E., Bowman, J.R., 1989. Development of Asian monsoon revealed by marked ecological shift during the latest Miocene in northern Pakistan. Nature 342, 163–166.

Rea, D.K., 1994. The paleoclimatic record provided by eolian deposition in the deep-sea: the geologic history of wind. Rev. Geophys. 32, 159–195.

Retallack, G.J., 2007. Cenozoic paleoclimate on land in North America. J. Geol. 115, 271–294.

Revenga, C., Murray, S., Abramovitz, J., Hammond, A., 1998. Watersheds of the World: Ecological Value and Vulnerability. World Resources Institute, Washington, DC.

Roden, J.S., Lin, G., Ehleringer, J.R., 2000. A mechanistic model for interpretation of hydrogen and oxygen isotope ratios in tree-ring cellulose. Geochim. Cosmochim. Acta 64 (1), 21–35.

Rommerskirchen, F., Plader, A., Eglinton, G., Chikaraishi, Y., Rullkotter, J., 2006. Chemotaxonomic significance of distribution and stable carbon isotopic composition of long-chain alkanes and alkan-1-ols in C_4 grass waxes. Org. Geochem. 37, 1303–1332.

Ruddiman, W.F., Prell, W.L., Raymo, M.E., 1989. Late Cenozoic uplift in southern Asia and the American West: rationale for general circulation modeling experiments. J. Geophys. Res. 94, 18379–18391.

Russell, J.M., McCoy, S.J., Verschuren, D., Bessems, I., Huang, Y., 2009. Human impacts, climate change, and aquatic ecosystem response during the past 2000 yr at Lake Wandakara, Uganda. Quatern. Res. 72 (3), 315–324.

Sachse, D., Radke, J., Gleixner, G., 2006. dD values of individual n-alkanes from terrestrial plants along a climatic gradient – Implications for the sedimentary biomarker record. Org. Geochem. 37 (4), 469–483.

Sachse, D., Kahmen, A., Gleixner, G., 2009. Significant seasonal variation in the hydrogen isotopic composition of leaf-wax lipids for two deciduous tree ecosystems (Fagus sylvativa and Acer pseudoplatanus). Org. Geochem 40, 732–742.

Sage, R.F., 2004. The evolution of C_4 photosynthesis. New Phytol. 161, 341–370.

Schefuss, E., Ratmeyer, V., Stuut, J.B.W., Jansen, J.H.F., Sinninghe Damste, J.S., 2003. Carbon isotope analyses of *n*-alkanes in dust from the lower atmosphere over the central eastern Atlantic. Geochim. Cosmochim. Acta 67, 1757–1767.

Segalen, L., et al., 2006. Neogene climate change and emergence of C_4 grasses in the Namib, southwestern Africa, as reflected in ratite ^{13}C and ^{18}O. Earth Planet. Sci. Lett. 244, 725–734.

Sepulchre, P., et al., 2006. Tectonic uplift and eastern Africa aridification. Science 313, 1419–1423.

Shunk, A.J., Driese, S.G., Clark, G.M., 2006. Latest Miocene to earliest Pliocene sedimentation and climate record derived from paleosinkhole fill deposits, Gray Fossil Site, northeastern Tennessee, U.S.A. Palaeogeogr. Palaeoclimatol. Palaeoecol. 231 (3–4), 265–278.

Shunk, A.J., Driese, S.G., Dunbar, J.A., 2009. Late Tertiary paleoclimatic interpretation from lacustrine rhythmites in the Gray Fossil Site, northeastern Tennessee, USA. J. Paleolimnol. 42 (1), 11–24.

Simoneit, B.R.T., 1997. Compound-specific carbon isotope analysis of individual long-chain alkanes and alkanoic acids in Harmatten aerosols. Atmos. Environ. 31 (15), 2225–2233.

Sloane, B.J., 1971. Recent developments in the Miocene Planulina gas trend of south Louisiana. Gulf Coast Assoc. Geol. Soc. Trans. 21, 199–210.

Smith, G.R., 1994. Climatic influences on continental deposition during late-stage filling of an extensional basin, southeastern Arizona. Geol. Soc. Am. Bull. 106, 1212–1228.

Smith, F.A., Freeman, K.H., 2006. Influence of physiology and climate on δD of leaf wax *n*-alkanes from C_3 and C_4 grasses. Geochim. Cosmochim. Acta 70, 1172–1187.

Smith, G.R., Patterson, W.P., 1994. Mio-Pliocene seasonality on the Snake River Plain: comparison of faunal and oxygen isotope evidence. Palaeogeogr. Palaeoclimatol. Palaeoecol. 107 (3–4), 291–302.

Smith, G.R., Wang, Y., Cerling, T.E., Geissman, J.W., 1993. Comparison of Paleosol-carbonate isotope record to other records of Pliocene–Early Pleistocene climate in the western United States. Geology 21 (691–694).

Smittenberg, R.H., et al., 2004. Compound-specific radiocarbon dating of the varved Holocene sedimentary record of Saanich Inlet, Canada. Paleoceanography 19 (2) PA2012.

Snyder, S.W., Mauger, L.L., Ames, D., 2001. Benthic foraminifera and paleoecology of the Pliocene Yorktown and Chowan River Formations, Lee Creek Mine, North Carolina, USA. J. Foramin. Res. 31 (3), 244–274.

Strömberg, C.A.E., 2005. Decoupled taxonomic radiation and ecological expansion of open-habitat grasses in the Cenozoic of North America. Proc. Natl Acad. Sci. U. S. A. 102, 11980–11984.

Thompson, R.S., 1991. Pliocene environments and climates in the western United States. Quatern. Sci. Rev. 10, 115.

Tierney, J.E., Russell, J.M., Huang, Y., 2010. A molecular perspective on Late Quaternary climate and vegetation change in the Lake Tanganyika basin, East Africa. Quatern. Sci. Rev. 29 (5–6), 787–800.

Tipple, B.J., Pagani, M., 2007. The early origins of terrestrial C_4 photosynthesis. Annu. Rev. Earth Planet. Sci. 35, 435–461.

Tipple, B.J., Meyers, S.R., Pagani, M., 2010. The carbon isotope ratio of Cenozoic CO_2: a comparative evaluation of available geochemical proxies. Paleoceanography PA001851.

Trefry, J.H., Metz, S., Nelsen, T.A., Trocine, R.P., Eadie, B.J., 1994. Transport of particulate organic carbon by the Mississippi River and its fate in the Gulf of Mexico. Estuaries 17, 839–849.

Vellinga, M., Wood, R.A., 2002. Global climatic impacts of a collapse of the Atlantic thermohaline circulation. Clim. Change 54, 251–267.

Vincentini, A., Barber, J.C., Aliscioni, S.S., Giussanis, L.M., Kellogg, E.A., 2008. The age of the grasses and clusters of origins of C_4 photosynthesis. Global Change Biol. 14, 2963–2977.

Vogts, A., Moossen, H., Rommerskirchen, F., Rullkotter, J., 2009. Distribution patterns and stable carbon isotopic composition of alkanes and alkan-1-ols from plant waxes of African rain forest and savanna C_3 species. Org. Geochem. 40, 1037–1054.

Wakeham, S.G., Pease, T.K., 1992. Lipid Analysis in Marine Particles and Sediment Samples. Skidaway Institute of Oceanography, Savannah, GA.

Waterson, E.J., Canuel, E.A., 2008. Sources of sedimentary organic matter in the Mississippi River and adjacent Gulf of Mexico as revealed by lipid biomarker and $\delta^{13}C_{TOC}$ analyses. Org. Geochem. 39, 422–439.

Winker, C.D., 1981. Cenozoic shelf margins, northwestern Gulf of Mexico. In: Perkins, B.F., Ventress, W.P.S., Edwards, M.B. (Eds.), Recognition of shallow-water versus deep-water sedimentary facies in growth-structure-affected formations of the Gulf Coast Basin. 2nd Annual Research Conference, Program and Abstracts. Society of Economic Paleontologists and Mineralogists, Gulf Coast Section, pp. 74–82.

Wolfe, J.A., 1994. Tertiary climate changes at middle latitudes of western North America. Palaeogeogr. Palaeoclimatol. Palaeoecol. 108, 195–205.

Worzel, J.L., et al., 1971. Site 94. Initial Reports of the Deep Sea Drilling Project, Leg 10. Deep Sea Drilling Project, Washington, D.C, pp. 195–258.

Yang, S., Ding, X., Zheng, D., Li, Q., 2007. Depiction of the variations of Great Plains precipitation and its relationship with tropical central-eastern Pacific SST. J. Appl. Meteorol. Climatol. 46 (2), 136–153.

Zachos, J.C., Pagani, M., Sloan, L., Thomas, E., Billups, K., 2001. Trends, rhythms, and aberrations in global climate 65 Ma to present. Science 292 (5517), 686–693.

Zhang, P., Molar, P., Downs, W.R., 2001. Increased sedimentation rates and grain sizes 2–4 Myr ago due to the influence of climate change on erosion rates. Nature 410, 891–897.